Award Number: W81XWH-10-1-0951

TITLE: Effect of Teriparatide, Vibration and the Combination on Bone Mass and Bone Architecture in Chronic Spinal Cord Injury

PRINCIPAL INVESTIGATOR: Thomas J. Schnitzer, MD, PhD

CONTRACTING ORGANIZATION: Northwestern University
Evanston, IL 60208

REPORT DATE: December 2015

TYPE OF REPORT: Final Report

PREPARED FOR: U.S. Army Medical Research and Materiel Command
Fort Detrick, Maryland 21702-5012

DISTRIBUTION STATEMENT:

☑ Approved for public release; distribution unlimited

REPORT DOCUMENTATION PAGE

Form Approved
OMB No. 0704-0188

1. REPORT DATE *(DD-MM-YYYY)*	2. REPORT TYPE	3. DATES COVERED *(From - To)*
December 2015	Final Report	27 Sep 2010-26 Sep 2015

4. TITLE AND SUBTITLE
Effect of Teriparatide, Vibration and the Combination on Bone Mass and Bone Architecture in Chronic Spinal Cord Injury

5a. CONTRACT NUMBER
W81XWH-10-1-0951

5b. GRANT NUMBER
n/a

5c. PROGRAM ELEMENT NUMBER

6. AUTHOR(S)
Thomas J. Schnitzer, MD, PhD

email: tjs@northwestern.edu

5d. PROJECT NUMBER

5e. TASK NUMBER

5f. WORK UNIT NUMBER

7. PERFORMING ORGANIZATION NAME(S) AND ADDRESS(ES)
Northwestern University
633 Clark St.
Evanston,IL 60208-0001

8. PERFORMING ORGANIZATION REPORT NUMBER

9. SPONSORING / MONITORING AGENCY NAME(S) AND ADDRESS(ES)
US Army Medical Research and Materiel Command
Fort Detrick, MD 21702-5012

10. SPONSOR/MONITOR'S ACRONYM(S)

11. SPONSOR/MONITOR'S REPORT NUMBER(S)

12. DISTRIBUTION / AVAILABILITY STATEMENT
Approved for public release; distribution unlimited

13. SUPPLEMENTARY NOTES

14. ABSTRACT
Severe bone loss commonly occurs in individuals with chronic spinal cord injury who are non-weight-bearing and leads to an increased risk of lower extremity fractures. This 12 month, multi-site, double-blind, randomized, placebo-controlled study evaluates the efficacy and safety of two interventions known to be anabolic to bone, parathyroid hormone and mechanical loading (provided as teriparatide and vibration, respectively) in 60 SCI individuals with low bone mass. 56 out of 60 participants (retention rate of 93%) completed the initial treatment period (1 year); 24 of 25 participants who elected to enter a 1 year open-label extension of teriparatide therapy have recently completed. No safety issues have arisen during the course of the study. The data from the first year of treatment show no statistically significant difference among the 3 treatment groups in bone density or bone strength at any skeletal site despite bone marker data demonstrating a metabolic response to teriparatide but not to vibration alone. Results from the second year of treatment are not yet available.

15. SUBJECT TERMS
Spinal cord injury, bone density, osteoporosis, teriparatide, vibration

16. SECURITY CLASSIFICATION OF:			17. LIMITATION OF ABSTRACT	18. NUMBER OF PAGES	19a. NAME OF RESPONSIBLE PERSON
a. REPORT	b. ABSTRACT	c. THIS PAGE			USAMRMC
U	U	U	UU	51	19b. TELEPHONE NUMBER *(include area code)*

Standard Form 298 (Rev. 8-98)
Prescribed by ANSI Std. Z39.18

Table of Contents

Page

INTRODUCTION:

Acute spinal cord injury (SCI) is associated with subsequent rapid and profound bone loss, particularly in the lower extremities of individuals who are not weight-bearing.[1, 2] Bone loss continues at an accelerated rate for the next 2-5 years and then a new steady-state is reached for bone turnover with stable but markedly reduced (50%-70%) bone mass in the distal femur and proximal tibia.[3] This reduced bone mass results in a documented increase in risk for lower extremity fracture and an associated increase in morbidity and health care costs in this population.[4-6] Currently, few people with SCI are being treated, one argument being that treatment is not effective and fractures are not disabling in a non-ambulatory population. Because of the magnitude of the bone loss in chronic SCI and the fact that enhanced bone resorption is not the primary problem in maintaining bone loss in chronic SCI, the focus for increasing bone mass needs to be on anabolic agents. Parathyroid hormone, when given on an intermittent basis, is an agent that is markedly anabolic and has been shown to be effective in able-bodied individuals in increasing bone mass, bone quality and preventing fractures[7-9], but has not been studied in chronic SCI. In animal studies, PTH increases bone mass in models of disuse-mediated bone loss, a condition similar to that of SCI in man[10, 11]. Furthermore, PTH efficacy has been shown to be enhanced, in a synergistic manner, when combined with mechanical loading under these conditions[12-14]. Thus, an approach that utilizes both of these anabolic modalities in chronic SCI would provide the optimal opportunity to see an increase in bone mass. Mechanical loading in people with SCI is difficult to achieve due to their limited ability to bear weight, but application of vibrational forces to deliver mechanical loads have been shown to be an anabolic bone stimulus, effective in increasing bone mass in animals and man[15-17]. Thus, we proposed to investigate PTH, in the form of teriparatide, the commercially available product, and directed vibration to assess their ability to increase bone mass in individuals with SCI.

KEYWORDS: spinal cord injury, bone loss, bone mass, bone strength, osteoporosis, teriparatide, mechanical vibration

OVERALL PROJECT SUMMARY:

Study Aims:

AIM 1: To determine if a potent anabolic agent, PTH, provided as teriparatide, and mechanical loading, provided by means of vibration, alone or together will increase bone mass after 12 months of treatment in people with chronic SCI and lower extremity bone loss.

AIM 2: To evaluate the effects of teriparatide and vibration, individually and together, on bone microarchitectural parameters in people with chronic SCI and bone loss.

AIM 3: To evaluate the mechanism by which teriparatide and vibration, individually and together, affect bone metabolism by measuring markers of bone metabolism in patients with chronic SCI.

Study Design:

This study evaluates the ability of two interventions, parathyroid hormone and mechanical loading, separately and together, to increase bone mass in individuals with chronic SCI and low bone mass. These interventions have previously been shown to be effective in increasing bone mass and decreasing fractures in non-disabled populations of men and post-menopausal women but have not been examined in individuals with SCI. In this three-arm, modified factorial design, double-blind, placebo-controlled study, 60 people with chronic SCI received daily teriparatide and mechanical vibration. Assessment of bone mass (by DXA scanning and quantitative computed tomography and bone metabolism (by serum

bone markers) has been undertaken at baseline and at regular intervals during one year of treatment to permit evaluation of the efficacy of these interventions. A one year open-label extension was offered to all participants completing the study during which treatment with daily teriparatide and mechanical vibration occurred. The same outcome measures were assessed every 6 months during this second treatment period. Subjects completing the second year of teriparatide were given the opportunity to enroll in a final year of oral alendronate 70mg weekly with outcome measures again measured each 6 months.

Study Results: Demographics and baseline clinical data

61 participants were randomized (50 at the Northwestern/RIC site and 11 at the Hines VA site) and 60 received study intervention (49 at the Northwestern/RIC site and 11 at the Hines VA site) at two sites in this clinical study. 56 participants were able to be evaluated at 12 months (93% retention), with 4 participants lost to follow-up (see appendix B). The group was predominantly male (82%), with an even mix of Caucasian and African-Americans. Mean age was 45.7 years.

Table 1. Demographic and baseline clinical data

Demographic Data	
Mean Age (yr, SD)	45.7 ± 16.7
Sex	49M/11F
Ethnicity	48 Not Hispanic or Latino, 12 Hispanic or Latino
Race	29 White, 28 Black, 2 Native Hawaiian/Other, 1 Asian
BMI	24.9 ± 6.2
Clinical Descriptors	
Time post-SCI (yr, SD)	18.9 ± 13.8
Injury Level (cervical/thoracic/lumbar)	19 C/39 Th/ 2 L
Motor Complete/Incomplete	46 Complete/14 Incomplete

Study Results: Changes in bone mass (DXA-determined BMD) after 12 months

After one year of treatment with teriparatide plus vibration, teriparatide alone and vibration alone, there was a statistically significant increase ($p < 0.05$) from baseline in the DXA-determined BMD at the lumbar spine in the groups receiving teriparatide whereas the vibration group alone showed no increase. The differences in BMD at the spine at one year between the teriparatide alone group and the teriparatide plus vibration group compared to the vibration group alone approached but did not reach statistical significance ($p = 0.08$ for both). BMD at the spine increased in a linear manner over time (Figure 1). At the hip, there was an apparent small increase in BMD in the groups receiving teriparatide at 6 months which showed no further increase with additional treatment. The group receiving vibration alone showed a small non-significant decrease in BMD at 6 months which returned to baseline values by 12 months. At the 12 month time point, there was no significant difference between any of the groups, and no significant change from baseline in BMD (Table 2). Similar findings were observed by DXA at the knee skeletal sites (distal femur, proximal tibia).

Figure 1: BMD change (mean±SE) over time at the spine and hip

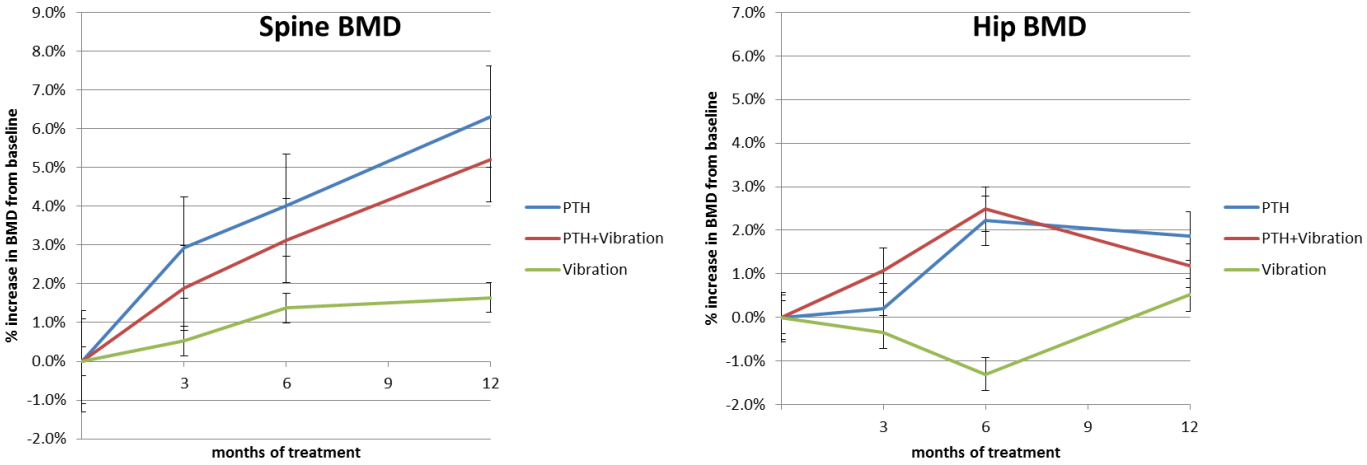

Table 2: BMD change over time at the spine and hip

	Δ Spine BMD			Δ Hip BMD		
	3 mo	6 mo	12 mo	3 mo	6 mo	12 mo
PTH	2.9%	4.0%	6.3%	0.2%	2.2%	1.9%
PTH+vibration	1.9%	3.1%	5.2%	1.1%	2.5%	1.2%
Vibration	0.5%	1.4%	1.6%	-0.3%	-1.3%	0.5%

Study Results: Changes in integral, trabecular, and cortical bone mass at the knee over 12 months (CT)

CT evaluation of bone at the knee demonstrated no significant changes in integral (Figure 2), trabecular (Figure 3), or cortical (Figure 4) bone mineral content over the 12 months of treatment in any group (see Appendix C for description of methodology). There was considerable variability in the measurements but no trend for change.

Figure 2. Absolute change in integral bone mineral content over time.

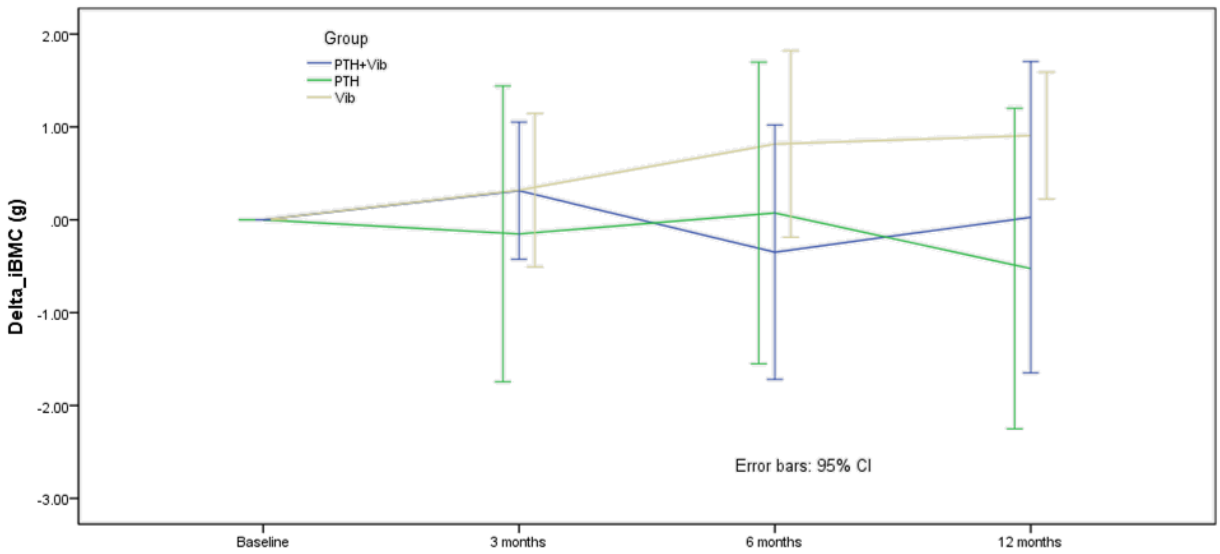

Figure 3. Absolute change in trabecular bone mineral content over time.

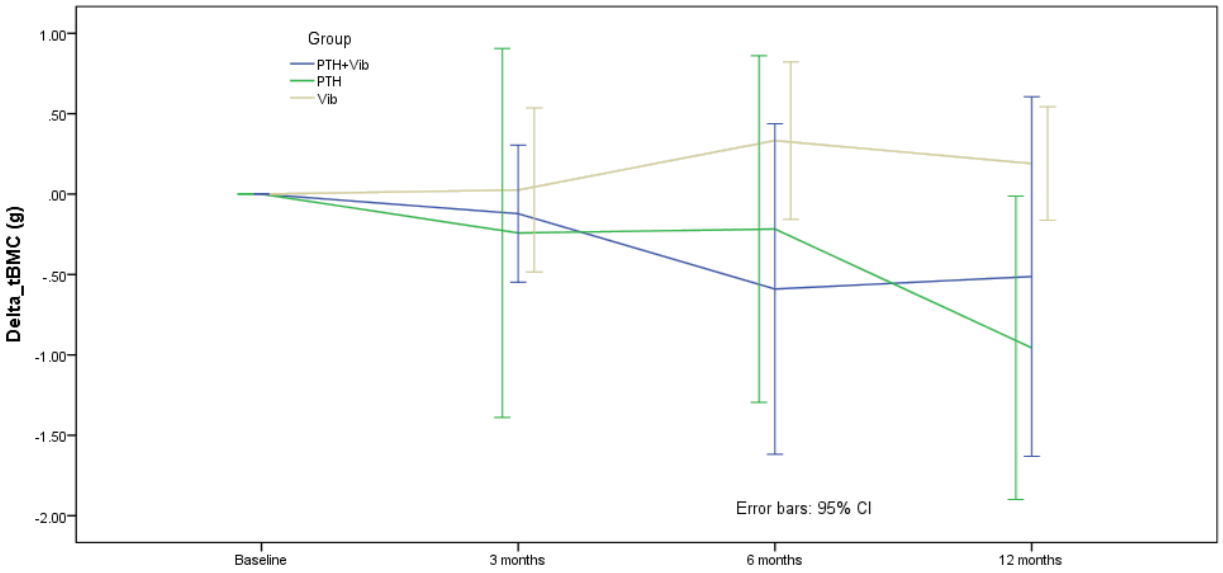

Figure 4. Absolute change in cortical bone mineral content over time.

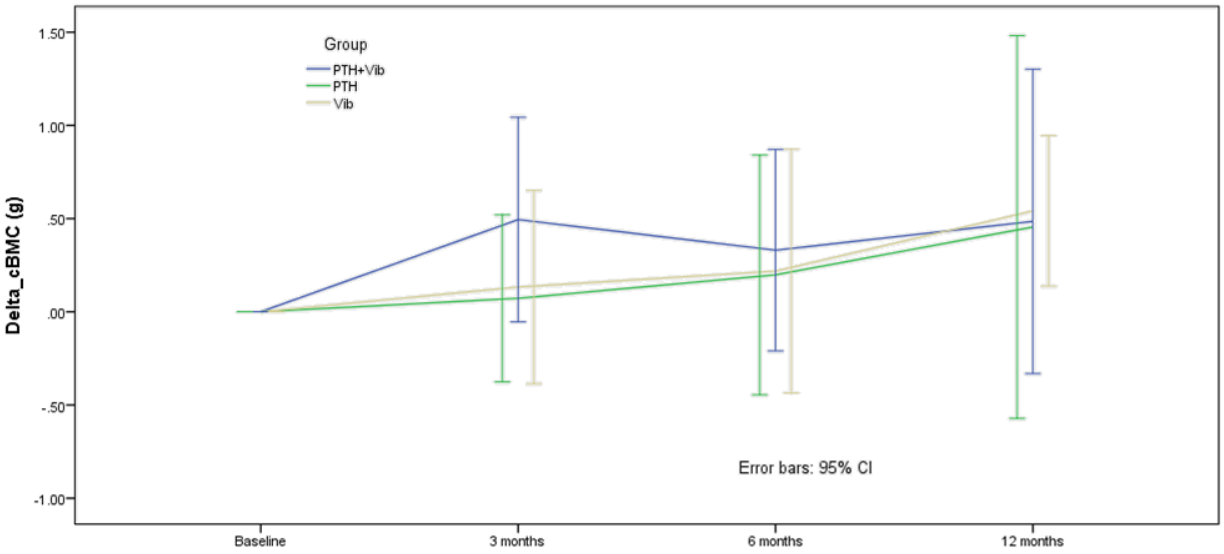

Study Results: Changes in DXA-determined BMD at the distal femur and proximal tibia

Measurements of BMD by DXA at the distal femur and proximal tibia (Fig. 5) showed relatively small changes over time. There was a great deal of variability in these measurements and no statistically significant difference at any time points. There may be slight suggestion of an effect by PTH+vibration, particularly after 6 months, but the variability in these measures makes it difficult to have confidence that any real differences were seen.

Figure 5: DXA BMD change (mean±SE) over time at the distal femur and proximal tibia

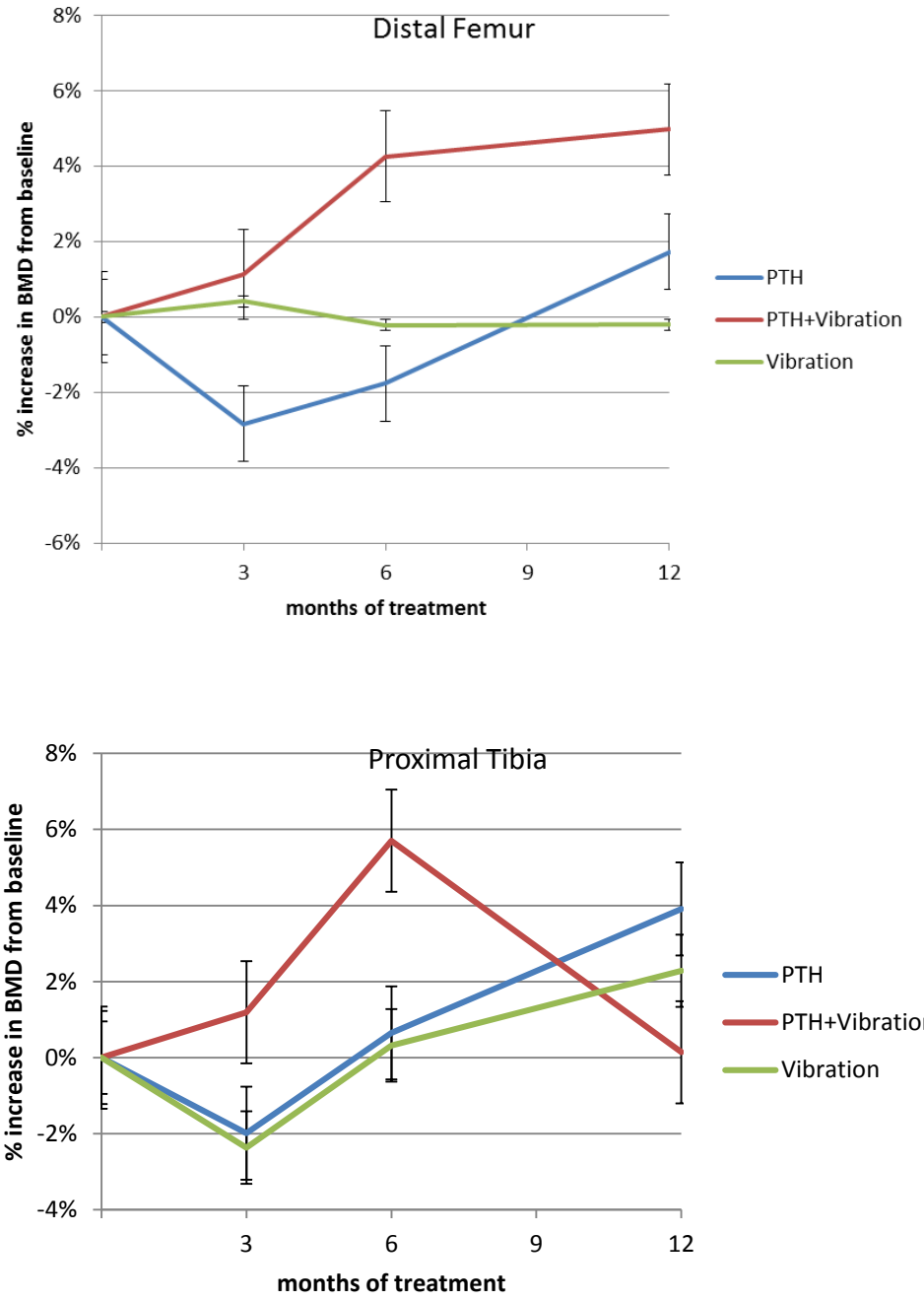

Study Results: Changes in serum levels of bone markers over 12 months

In the groups receiving teriparatide, there was a rapid and significant increase from baseline in the median serum levels of markers of both P1NP and CTX, markers of bone formation and resorption. In the group receiving vibration alone there was no significant change. Changes in BSAP were less marked than those seen for P1NP but were directionally similar and paralleled the differences in group changes seen with the other markers. In the groups receiving teriparatide, the increase in the bone formation marker P1NP was greatest in the first 3-6 months and then decreased by 12 months whereas the bone resorption marker CTX tended to remain elevated throughout (see Fig.6).

Figure 6. Change in serum markers (mean±SE) of bone metabolism over time

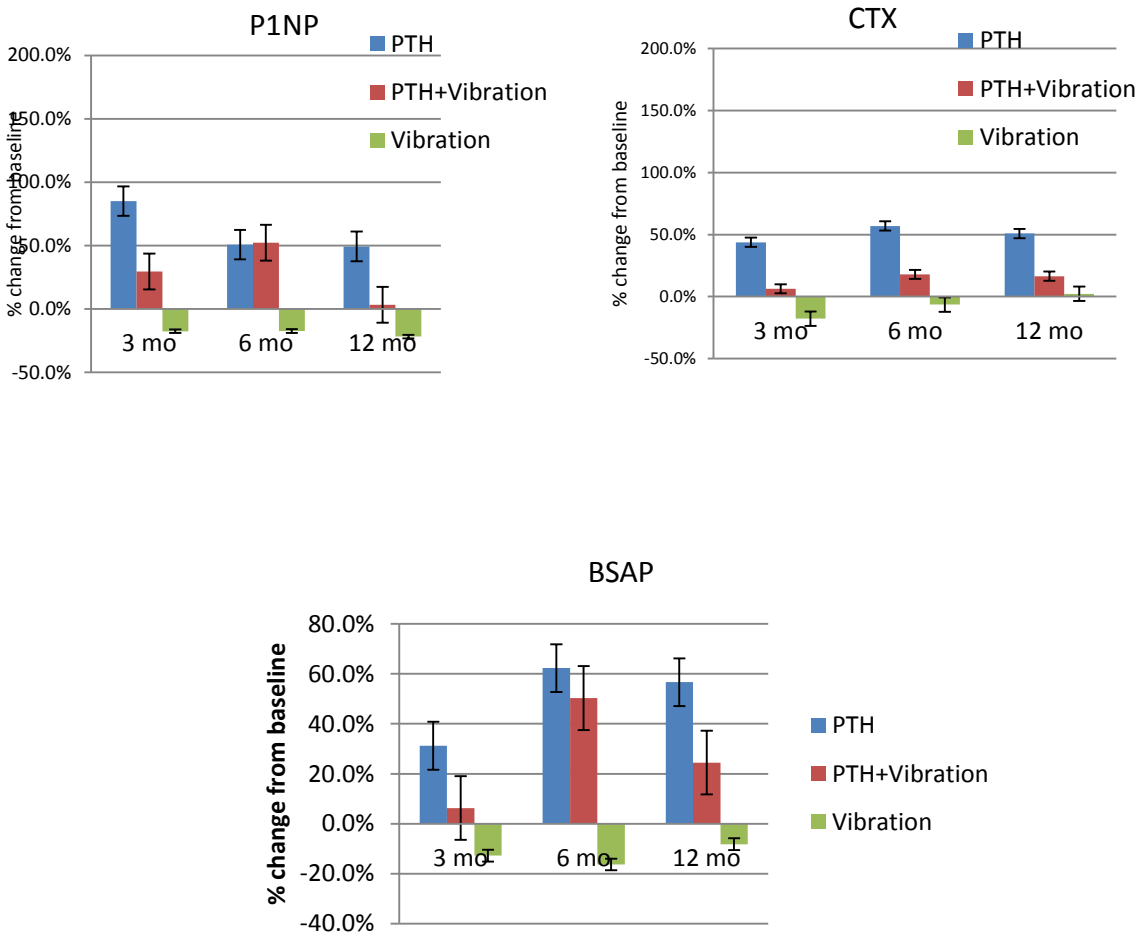

Study Results: Changes in BMD, integral and trabecular bone density and serum levels of bone markers between 12 and 24 months

The database for these data points is being cleaned and serum sample results are pending. Analyses will be completed in the coming months.

Study Results: Safety

Safety was assessed by open-ended interviews of subjects at each contact, which included all clinic visits and when contact was made by telephone. Adverse event reporting was done based on GCP guidelines. A medical monitor reviewed all adverse events and regularly scheduled data safety monitoring meetings occurred. These were scheduled for every 6 months but increased in frequency during the course of the trial due to the report of a number of fractures. Upon blinded review, the fracture incidence appeared to be similar in all 3 treatment groups. Fracture incidence declined during the remainder of the study. No other adverse events were reported at rates greater than what would be expected in this population.

KEY RESEARCH ACCOMPLISHMENTS:

- 56 participants of 60 who were originally randomized and treated were followed for the full year of treatment. Retention rate was 93%.
- Teriparatide administration at 20 ug/day for 12 months results in a significant increase in BMD measured by DXA at the spine in individuals after SCI.
- Teriparatide has no clinically or statistically significant effect on BMD measured by DXA or CT at the hip or the knee after 12 months' treatment.
- Individuals receiving teriparatide demonstrated a biologic response to teriparatide treatment as serum levels of anabolic and catabolic bone markers, P1NP and CTX respectively, were elevated with teriparatide treatment.
- Vibration treatment has no effect alone, or with teriparatide, on bone response determined by either measurement of BMD by DXA or CT or on serum levels of bone markers.
- No safety issues were identified in any of the treatment groups.

CONCLUSION:

Teriparatide, a potent bone anabolic agent, did increase bone density at the spine in individuals after SCI. However, at other skeletal sites, particularly the hip and knee, there was no effect of treatment with teriparatide, vibration or the combination on bone density, measured by DXA or CT. These latter skeletal sites are clinically the most important as fractures are most prevalent at these areas in individuals with SCI. The fact that serum levels of bone markers responded to teriparatide treatment demonstrates that this treatment did result in a biologic effect (also evident at the spine) but that this response either was not occurring or was not detectable at other skeletal sites. Vibration alone, or in combination with teriparatide, did not result in any additional change in bone density or in serum markers of bone metabolism, supporting the fact that it was not effective in this setting.

The failure to detect a response to teriparatide is disappointing but not surprising, given the fact that response to PTH is known to be highly dependent on normal bone loading which was absent in these participants.[12-14] Vibration treatment was not able to substitute for normal mechanical loading in this setting. Additionally, it should be noted that teriparatide alone after 12 months may not result in a measurable increase in hip BMD, even in able-bodied osteoporotic individuals[18], and hence the effects that were seen in this study are completely consistent with a biologic response to teriparatide, but without detectable change in BMD at the hip. Changes in BMD at the knee, including both trabecular and cortical areas, were not evident but the sensitivity of the CT measurement may not have been adequate to detect small changes. What is clear is that there were no major changes – similar in magnitude to those seen at the spine – evident at the knee in these participants.

The optimal period of time to treat participants with teriparatide is not known. Teriparatide is approved for 2 years of treatment, and additional increases in BMD may occur with further use[19]. Thus, an extension study was initiated to determine whether a second year of teriparatide treatment, followed by a year of alendronate therapy, could have a greater magnitude of effect at these skeletal sites. This study is currently still active and results are not yet available.

PUBLICATIONS, ABSTRACTS AND PRESENTATIONS:

Publications (to date)

1. Edwards, W.B., and Schnitzer, T.J. (2015). Bone imaging and fracture risk after spinal cord injury. Current Osteoporosis Reports, 13, 310-317.
2. Edwards, W.B., Troy, K.L., Simonian, N., and Schnitzer, T.J. (2015). Reduction in torsional stiffness and strength at the proximal tibia as a function of time since spinal cord injury. Journal of Bone and Mineral Research, 30, 1422-1430.
3. McPherson, J.G., Edwards, W.B., Prasad, A., Troy, K.L., Griffith, J.W., and Schnitzer, T.J. (2014). Dual energy x-ray absorptiometry of the knee in spinal cord injury: methodology and correlation with quantitative computed tomography. Spinal Cord, 52, 821-825.

Published Abstracts

1. Edwards, W.B., Simonian, N., & Schnitzer, T.J. (May, 2015). Bone mineral density assessed by QCT, but not DXA, discriminates SCI patients with prevalent fragility fractures. Proceedings of the 4th Joint Meeting of the ISCoS and ASIA, Montreal, Quebec.
2. Edwards, W.B., Simonian, N., Troy, K.L., & Schnitzer, T.J. (September, 2014). Discriminants of prevalent fragility fractures in chronic spinal cord injury. Proceedings of the American Society of Bone and Mineral Research Annual Meeting, Houston, Texas.
3. Butler, T., Schnitzer, T.J., Edwards, W.B., & Troy, K.L. (September, 2014). Increased marrow adipose tissue following spinal cord injury. Proceedings of the American Society of Bone and Mineral Research Annual Meeting, Houston, Texas.
4. Edwards, W.B., Simonian, N., Troy, K.L., & Schnitzer T.J. (August, 2014). Reduction in proximal tibia compartmental bone mineral as a function of time since spinal cord injury. Proceedings of the Internal Bone & Mineral Society's 43rd International Sun Valley Workshop: Musculoskeletal Biology, Sun Valley, Idaho.
5. Prasad, A., Edwards, W.B., Marks, J., Troy, K. L., Schnitzer, T. J. (May, 2014). Correlation of DXA and QCT imaging at the knee in adults with spinal cord injury. Proceedings of the ASIA 40th Annual Scientific Meeting, San Antonio, Texas.
6. Edwards, W.B., Schnitzer T.J., & Troy, K.L. (October, 2013). Changes in fracture strength as a function of time since spinal cord injury. Proceedings of the American Society of Bone and Mineral Research Annual Meeting, Baltimore, Maryland.
7. Prasad A., Edwards, W.B., Hermann, K., Barkema, D., Simonian, N., Yeasted, R., Troy, K.L., & Schnitzer T.J. (October, 2013). DXA vs QCT imaging of the knee in people with spinal cord injury. Proceedings of the American Society of Bone and Mineral Research Annual Meeting, Baltimore, Maryland.

Conference Presentations

1. Edwards, W.B., Simonian, N., & Schnitzer, T.J. (May, 2015). Bone mineral density assessed by QCT, but not DXA, discriminates SCI patients with prevalent fragility fractures. Proceedings of the 4th Joint Meeting of the ISCoS and ASIA, Montreal, Quebec.

INVENTIONS, PATENTS AND LICENSES:

Nothing to report.

REPORTABLE OUTCOMES:

Nothing to report.

OTHER ACHIEVEMENTS:

Nothing to report.

REFERENCES:

1. Jiang, S.D., L.Y. Dai, and L.S. Jiang, *Osteoporosis after spinal cord injury.* Osteoporos Int, 2006. **17**(2): p. 180-92.
2. Maimoun, L., et al., *Bone loss in spinal cord-injured patients: from physiopathology to therapy.* Spinal Cord, 2006. **44**(4): p. 203-10.
3. Frotzler, A., et al., *Bone steady-state is established at reduced bone strength after spinal cord injury: a longitudinal study using peripheral quantitative computed tomography (pQCT).* Bone, 2008. **43**(3): p. 549-55.
4. Lazo, M.G., et al., *Osteoporosis and risk of fracture in men with spinal cord injury.* Spinal Cord, 2001. **39**(4): p. 208-14.
5. Frisbie, J.H., *Fractures after myelopathy: the risk quantified.* J Spinal Cord Med, 1997. **20**(1): p. 66-9.
6. Logan, W.C., Jr., et al., *Incidence of fractures in a cohort of veterans with chronic multiple sclerosis or traumatic spinal cord injury.* Arch Phys Med Rehabil, 2008. **89**(2): p. 237-43.
7. Neer, R.M., et al., *Effect of parathyroid hormone (1-34) on fractures and bone mineral density in postmenopausal women with osteoporosis.* N Engl J Med, 2001. **344**(19): p. 1434-41.
8. Kurland, E.S., et al., *Parathyroid hormone as a therapy for idiopathic osteoporosis in men: effects on bone mineral density and bone markers.* J Clin Endocrinol Metab, 2000. **85**(9): p. 3069-76.
9. Zanchetta, J.R., et al., *Effects of teriparatide [recombinant human parathyroid hormone (1-34)] on cortical bone in postmenopausal women with osteoporosis.* J Bone Miner Res, 2003. **18**(3): p. 539-43.
10. Ma, Y., et al., *Parathyroid hormone and mechanical usage have a synergistic effect in rat tibial diaphyseal cortical bone.* J Bone Miner Res, 1999. **14**(3): p. 439-48.
11. Turner, R.T., et al., *Programmed administration of parathyroid hormone increases bone formation and reduces bone loss in hindlimb-unloaded ovariectomized rats.* Endocrinology, 1998. **139**(10): p. 4086-91.
12. Li, J., et al., *Parathyroid hormone enhances mechanically induced bone formation, possibly involving L-type voltage-sensitive calcium channels.* Endocrinology, 2003. **144**(4): p. 1226-33.
13. Kim, C.H., et al., *Trabecular bone response to mechanical and parathyroid hormone stimulation: the role of mechanical microenvironment.* J Bone Miner Res, 2003. **18**(12): p. 2116-25.
14. Hagino, H., et al., *Effect of parathyroid hormone on cortical bone response to in vivo external loading of the rat tibia.* J Bone Miner Metab, 2001. **19**(4): p. 244-50.
15. Rubin, C., et al., *Prevention of postmenopausal bone loss by a low-magnitude, high-frequency mechanical stimuli: a clinical trial assessing compliance, efficacy, and safety.* J Bone Miner Res, 2004. **19**(3): p. 343-51.
16. Ward, K., et al., *Low magnitude mechanical loading is osteogenic in children with disabling conditions.* J Bone Miner Res, 2004. **19**(3): p. 360-9.
17. Gilsanz, V., et al., *Low-level, high-frequency mechanical signals enhance musculoskeletal development of young women with low BMD.* J Bone Miner Res, 2006. **21**(9): p. 1464-74.
18. H.K., G., et al., *Romosozumab Administration Is Associated With Significant Improvements In Lumbar Spine and Hip Volumetric Bone Mineral Density and Content Compared With Teriparatide.* Arthritis and Rheumatology, 2015. **Abstract 863**: p. http://acrabstracts.org/abstract/romosozumab-administration-is-associated-with-significant-improvements-in-lumbar-spine-and-hip-volumetric-bone-mineral-density-and-content-compared-with-teriparatide/.
19. Obermayer-Pietsch, B.M., et al., *Effects of two years of daily teriparatide treatment on BMD in postmenopausal women with severe osteoporosis with and without prior antiresorptive treatment.* J Bone Miner Res, 2008. **23**(10): p. 1591-600.

APPENDICES:

Appendix A. List of personnel receiving salary

Appendix B. Reasons for Loss to Follow-Up

Appendix C. Methodology for DXA and CT acquisition and analysis and quantitation of bone markers

Appendix D. Copies of abstracts and publications

Appendix A. List of personnel receiving salary

Name	Title
Barkema,Danielle Deone	Research Project Coordinator
Chen, David	Co-Investigator
Edwards, W. Brent	Co-Investigator
Gordon,Keith Edward	Co-Investigator
Griffith,James W	Statistician
Hauber,Sara	Research Project Manager
Herrmann,Kristina Marie	Research Technologist 1
Lange,Amy Marie	Clinical Research Nurse
Leslie, AnJelique	Research Coordinator
Lipowski,Meghan Ruth	Research Project Coordinator
Marks,Julia Ann	Research Project Coordinator
McPherson,Jacob G	Post-Doctoral Fellow
Nigg,Narina Simonian	Coord Clinical Research 3
Odle, Cheryl	Research Coordinator
Padalabalanarayanan,Sangeetha	Research Project Coordinator
Parachuri, Rama	Co-Investigator
Roth,Elliot J	Clinical Monitor
Schnitzer,Thomas J	Principal Investigator
Stephens,Bernard Lonnelle	Recruitment Specialist
Troy, Karen	Co-Investigator
Yeasted,Renita Evonne	Research Project Manager

Appendix B. Reasons for Loss to Follow-Up

002 - Subject withdrew from study around 3 month visit due to difficulty commuting to site (lived a couple of hours away). Multiple attempts were made to schedule subject for final study visit; however, visit was never completed.

049 - Subject stopped returning phone calls after 9 month visit. Multiple attempts were made to schedule subject for final study visit; however, visit was never completed.

059 - Subject stopped study treatment around 6 month visit. Multiple attempts were made to reach the subject and schedule subject for final study visit; however, visit was never completed.

075 - Subject stopped study drug shortly after 3 month visit due to complicated health status and family matters. Multiple attempts were made to schedule subject for final study visit; however, visit was never completed.

Appendix C. Methodology for DXA and CT acquisition and analysis and quantitation of bone markers

DXA Acquisition and Analysis

The DXA scans were performed using a Hologic QDR 4500A (Hologic, Waltham, MA, USA); standard acquisition and analysis protocols were used to quantify areal bone mineral density (aBMD) of spine, femoral neck and total proximal femur regions bilaterally.(1) For knee aBMD acquisition, a modified forearm algorithm was elected for scan acquisition, with the imaging field comprising the distal 2/3 of the femur and the proximal 1/3 of the tibia. The distal femur was divided into 2 regions for analysis, the femoral epiphysis (R1) and the metaphysis (R2) with a separate region of interest for the proximal tibia (R3) as described in a previous publication.(2) During scans, participants were placed in a supine position and the lower limb was stabilized in full extension. When possible, duplicate scans were obtained. We performed calibrations of the machine prior to each subject visit using a spine phantom, air scans and tissue bar scans. The day-to-day coefficient of variation (CV) of the spine phantom over the testing period was 0.387% (n=315). The precision of the DXA measurements at the distal femur epiphysis, distal femur metaphysis and the proximal tibia has been previously published, with the root-mean-square (RMS) CV being 3.12%, 4.70% and 3.40%, respectively.(3) If heterotopic ossification was visualized within the region of interest, data from that skeletal site was not utilized. Similarly, regions of interest containing metallic objects were also excluded.

CT Acquisition

Computed tomography data were acquired for the non-dominant knee (i.e., contralateral to hand dominance) of each participant using a scan length that captured the proximal most 15 cm of the tibia. The CT scans were performed using a Sensation 64 Cardiac Scanner (Siemens Medical Systems, Forchheim, Germany) with acquisition settings of 120 kVp and 200 mAs. Images were reconstructed with a slice thickness of 1 mm and an in-plane pixel resolution of 0.352 mm. All scans included a phantom in the field of view with known calcium hydroxyapatite concentrations (QRM, Moehrendorf, Germany).

QCT mineral analysis

QCT mineral analysis of the proximal tibia was performed using established protocols. (2, 4) Briefly, CT data were imported to Mimics (Materialise, Leuven, Belgium) where images were re-aligned so that the axial direction corresponded to the long axis of the tibia; the mediolateral axis was defined by a line passing through the medial and lateral condyles of the tibia and the anterioposterior axis was oriented orthogonally. The CT Hounsfield units were converted to calcium hydroxyapatite density ρ_{ha} using a linear relationship established with the phantom. This process can result in negative ρ_{ha} values for voxels comprised primarily of marrow fat.(5)

Proximal tibiae were segmented from the aligned images using a ρ_{ha} threshold of 0.15 g/cm3 to identify the periosteal surface boundary. Integral volumetric bone mineral density (vBMD; g/cm3) and bone mineral content (BMC; g) were calculated for the total proximal tibia, defined as all voxels within the periosteal surface boundary. The total proximal tibia included the first 30% of segment length, as measured from the proximal end of the bone. Segment lengths were estimated from self-reported stature using the proportionality constants of Drillis and Contini as cited by Winter.(6)

Local measures of compartmental bone were computed for epiphyseal, metaphyseal, and diaphyseal regions of the proximal tibia corresponding to 0-10%, 10-20%, and 20-30% of segment length, respectively. Cortical and trabecular compartments were identified as previously described [Edwards et al., 2013; 2014].(2, 4) Local measures of cortical vBMD and BMC were computed for the epiphysis,

metaphysis and diaphysis. Local measures of trabecular vBMD and BMC were only computed for the epiphysis and metaphysis. In addition, integral and cortical bone volumes (BV; cm3) were quantified for each region and used as surrogate measures of periosteal and endosteal expansion, respectively.

Bone Markers

Serum was obtained at baseline and each subsequent visit and frozen at -70C until assessed for type 1 procollagen amino-terminal propeptide (P1NP), collagen type 1 cross-linked C-telopeptide (CTX) and bone-specific alkaline phosphatase (BSAP) by Maine Medical Research Institute, Scarborough, ME, utilizing iSIS Analyzer (Luminescence) system, Immunodiagnostic Systems, Inc, Scottsdale, AZ.

1. Gordon KE, Wald MJ, Schnitzer TJ. Effect of parathyroid hormone combined with gait training on bone density and bone architecture in people with chronic spinal cord injury. Pm R. 2013;5(8):663-71. Epub 2013/04/06.
2. Edwards WB, Schnitzer TJ, Troy KL. Bone mineral and stiffness loss at the distal femur and proximal tibia in acute spinal cord injury. Osteoporos Int. 2014;25(3):1005-15. Epub 2013/11/06.
3. McPherson JG, Edwards WB, Prasad A, Troy KL, Griffith JW, Schnitzer TJ. Dual energy X-ray absorptiometry of the knee in spinal cord injury: methodology and correlation with quantitative computed tomography. Spinal Cord. 2014;52(11):821-5. Epub 2014/07/16.
4. Edwards WB, Schnitzer TJ, Troy KL. Torsional stiffness and strength of the proximal tibia are better predicted by finite element models than DXA or QCT. J Biomech. 2013;46(10):1655-62. Epub 2013/05/18.
5. Marshall LM, Lang TF, Lambert LC, Zmuda JM, Ensrud KE, Orwoll ES. Dimensions and volumetric BMD of the proximal femur and their relation to age among older U.S. men. J Bone Miner Res. 2006;21(8):1197-206. Epub 2006/07/28.
6. Winter DA. Biomechanics and motor control of human movement. 2nd ed. New York: John Wiley & Sons, Inc.; 1990.

Appendix D. Copies of publications and abstracts

Publications (to date)

1. Edwards, W.B., and Schnitzer, T.J. (2015). Bone imaging and fracture risk after spinal cord injury. Current Osteoporosis Reports, 13, 310-317.
2. Edwards, W.B., Troy, K.L., Simonian, N., and Schnitzer, T.J. (2015). Reduction in torsional stiffness and strength at the proximal tibia as a function of time since spinal cord injury. Journal of Bone and Mineral Research, 30, 1422-1430.
3. McPherson, J.G., Edwards, W.B., Prasad, A., Troy, K.L., Griffith, J.W., and Schnitzer, T.J. (2014). Dual energy x-ray absorptiometry of the knee in spinal cord injury: methodology and correlation with quantitative computed tomography. Spinal Cord, 52, 821-825.

Published Abstracts

1. Edwards, W.B., Simonian, N., & Schnitzer, T.J. (May, 2015). Bone mineral density assessed by QCT, but not DXA, discriminates SCI patients with prevalent fragility fractures. Proceedings of the 4th Joint Meeting of the ISCoS and ASIA, Montreal, Quebec.
2. Edwards, W.B., Simonian, N., Troy, K.L., & Schnitzer, T.J. (September, 2014). Discriminants of prevalent fragility fractures in chronic spinal cord injury. Proceedings of the American Society of Bone and Mineral Research Annual Meeting, Houston, Texas.
3. Butler, T., Schnitzer, T.J., Edwards, W.B., & Troy, K.L. (September, 2014). Increased marrow adipose tissue following spinal cord injury. Proceedings of the American Society of Bone and Mineral Research Annual Meeting, Houston, Texas.
4. Edwards, W.B., Simonian, N., Troy, K.L., & Schnitzer T.J. (August, 2014). Reduction in proximal tibia compartmental bone mineral as a function of time since spinal cord injury. Proceedings of the Internal Bone & Mineral Society's 43rd International Sun Valley Workshop: Musculoskeletal Biology, Sun Valley, Idaho.
5. Prasad, A., Edwards, W.B., Marks, J., Troy, K. L., Schnitzer, T. J. (May, 2014). Correlation of DXA and QCT imaging at the knee in adults with spinal cord injury. Proceedings of the ASIA 40th Annual Scientific Meeting, San Antonio, Texas.
6. Edwards, W.B., Schnitzer T.J., & Troy, K.L. (October, 2013). Changes in fracture strength as a function of time since spinal cord injury. Proceedings of the American Society of Bone and Mineral Research Annual Meeting, Baltimore, Maryland.
7. Prasad A., Edwards, W.B., Hermann, K., Barkema, D., Simonian, N., Yeasted, R., Troy, K.L., & Schnitzer T.J. (October, 2013). DXA vs QCT imaging of the knee in people with spinal cord injury. Proceedings of the American Society of Bone and Mineral Research Annual Meeting, Baltimore, Maryland.

Curr Osteoporos Rep (2015) 13:310–317
DOI 10.1007/s11914-015-0288-6

Bone Imaging and Fracture Risk after Spinal Cord Injury

W. Brent Edwards[1] · **Thomas J. Schnitzer**[2]

Published online: 16 August 2015

Abstract Spinal cord injury (SCI) is characterized by marked bone loss and an increased risk of fracture with high complication rate. Recent research based on advanced imaging analysis, including quantitative computed tomography (QCT) and patient-specific finite element (FE) modeling, has provided new and important insights into the magnitude and temporal pattern of bone loss, as well as the associated changes to bone structure and strength, following SCI. This work has illustrated the importance of early therapeutic treatment to prevent bone loss after SCI and may someday serve as the basis for a clinical fracture risk assessment tool for the SCI population. This review provides an update on the epidemiology of fracture after SCI and discusses new findings and significant developments related to bone loss and fracture risk assessment in the SCI population based on QCT analysis and patient-specific FE modeling.

Keywords DXA · QCT · Finite element model · Disuse osteoporosis · Bone strength · Bone fracture · Spinal cord injury

This article is part of the Topical Collection on *Therapeutics and Medical Management*

✉ W. Brent Edwards
wbedward@ucalgary.ca

[1] Human Performance Laboratory, Faculty of Kinesiology, and Division of Physical Medicine and Rehabilitation, Department of Clinical Neurosciences, Cumming School of Medicine, University of Calgary, 2500 University Dr. NW, Calgary, AB T2N 1N4, Canada

[2] Department of Physical Medicine and Rehabilitation, and Department of Internal Medicine, Division of Rheumatology, Northwestern University Feinberg School of Medicine, 303 E Chicago Ave, Chicago, IL 60611, USA

Introduction

Spinal cord injury (SCI) is characterized by rapid and profound bone loss from sublesional skeletal regions [1, 2]. This bone loss is believed to result from a combination of immobilization and neurogenic factors, but metabolic, endocrine, and vascular changes after SCI have also been implicated as important mediating factors [3, 4]. The degree of motor impairment plays an important role in SCI-related bone loss. Individuals with motor complete SCI tend to lose more bone than those with motor incomplete SCI [5, 6], and upper-extremity bone loss is unaffected in paraplegics and variably affected in quadriplegics, depending on the level and severity of injury [7, 8]. The clinical consequence of bone loss after SCI is an increased risk of skeletal fracture, often associated with little to no trauma [9, 10]. The impact of these fractures have on quality of life and functional ability, and the utilization of medical resources has been well documented [11, 12].

The pathogenesis of bone loss after SCI has been described in numerous review papers, as has the efficacy of pharmaceutical and non-pharmaceutical treatments to reduce or mitigate bone loss in this population. In fact, we are aware of some 25 reviews that have discussed these topics to some degree in the past decade (for comprehensive reviews see: [3, 13–21]). Despite the fact that bone loss after SCI is a well-established and highly discussed phenomenon, little progress has been made to reduce bone loss and the incidence of fracture observed after SCI, especially when compared to advancements made in postmenopausal and age-related osteoporosis [22]. In part, this is because there is still no standard of care for the detection, prevention, or treatment of SCI-related bone loss.

New research based on advanced imaging analysis, including quantitative computed tomography (QCT) and patient-specific finite element (FE) modeling, has provided new and important insights into the magnitude and temporal pattern of

bone loss, as well as the associated changes to bone structure and strength, following SCI. This technology has illustrated the importance of early (i.e., <1 year of injury) therapeutic treatment to prevent bone loss after SCI and may someday serve as the basis for a clinical fracture risk assessment tool specific to the SCI population. In this review, we provide an update on the epidemiology of fracture after SCI and discuss new findings and significant developments related to bone loss and fracture risk assessment in the SCI population based on QCT analysis and patient-specific FE modeling.

Fragility Fracture after SCI

Bone loss following SCI is associated with an increased risk of fracture, particularly low-energy, or fragility, fractures caused by minimal to no trauma. Although many individuals with SCI are non-ambulatory, these fractures remain a serious concern threatening quality of life and functional ability. More than 50 % of fracture-related hospitalizations are characterized by medical complications [11, 12] such as fracture non-union, delayed healing, and pressure ulcers from bracing and bed rest [11, 12, 23–28]. The duration of hospitalization for fracture-related admissions is seven times longer than non-fracture-related admissions with a higher rate of discharge to a second facility rather than home [11]. Together these factors result in significantly increased medical costs, loss of independence, and mortality [11, 29••, 30].

Despite the prevalence and severity of fractures after SCI, knowledge in this area is extremely lacking with data mostly coming from small cross-sectional studies and case reports. Coincident with the observed losses in bone mineral, fracture risk appears to be higher in individuals with motor complete SCI compared to those with motor incomplete SCI [11, 12, 24, 31, 32•]. Paraplegics have an increased risk of fracture relative to quadriplegics [27, 33, 34], most likely due to the increased levels of activity and independence. Although it has been estimated that as many as 50 % of individuals with SCI will experience a fracture at some point in their life [18], the exact incidence rate and prevalence of fragility facture after SCI remain unknown; a long-term prospective fracture surveillance study has never been conducted in the SCI population. Cross-sectional studies suggest a rate of fracture in the range of 1.2 to 3.4 per 100 patient years at risk [10–12, 27, 29••, 31, 35, 36], which is quite similar to the rate of non-vertebral fractures observed in postmenopausal osteoporotic women [37, 38].

The cause and location of fragility fracture after SCI have been documented qualitatively, though not in significant detail. Commonly reported causes of fracture after SCI include falls from wheelchairs, transfer activities, and non-traumatic events such as stretching or rolling over in bed [10, 11, 24, 27, 32•, 39]. Fractures after SCI have also occurred during active therapy protocols designed to strengthen the musculoskeletal system [40, 41], thereby limiting the degree to which functional declines can be reversed or attenuated. Unlike individuals with primary osteoporosis, fractures after SCI most frequently occur around regions of the knee, accounting for approximately 50 % of the fractures in this population (range 30–70 % [5, 10, 24–26, 31, 33]). Spiral fractures are often observed around the distal femur and proximal tibia [42, 43], implicating torsional loading as the principal mode of failure. We have also observed comminuted or impacted fracture patterns at the epiphyses of the distal femur and proximal tibia coincident with compressive or bending modes of loading. Proximal femoral fractures account for approximately 10 to 20 % of all fractures in this population [5, 31, 33], but they are among the most difficult to manage [11, 25, 26, 39]. These fractures typically occur after a fall from a wheelchair, or in the case of incomplete SCI, a fall from standing height or lower [44].

Duration of SCI has been shown to be a significant predictor of prevalent fracture [12, 29••, 32•, 36], simply meaning that individuals that have been injured for a longer period of time (i.e., longer exposure) are more likely to have experienced a fracture. The mean time to first fracture ranges between approximately 6 to 9 years of SCI [5, 10, 12, 27, 33], but has been reported to occur anywhere between 1 and 50 years after SCI [23, 36]. In these studies, the mean age at SCI was less than 35 years indicating that fractures after SCI occur at a much younger age when compared to individuals with primary osteoporosis. The increased incidence of fracture relative to the general population is observed after 3 years of injury [9], which corresponds well with the magnitude and temporal pattern of bone loss after SCI.

Bone Loss and Imaging after SCI

Much of what is known regarding bone loss after SCI comes from studies utilizing dual energy x-ray absorptiometry (DXA). However, DXA is limited to an areal projection or two-dimensional, measure of integral bone mineral at a region of interest. DXA cannot account for "true" changes in volumetric measures of bone mineral or changes to trabecular- and cortical-specific bone. The former limitation in areal bone mineral density (aBMD) manifests as an underestimation in changes to volumetric bone mineral density (vBMD) [45••], whereas the latter limitation is important because trabecular- and cortical-specific bone each make unique contributions to bone strength [46, 47] and respond quite differently to bone loss therapy [48, 49]. The information outlined in the section below comes from studies utilizing QCT analysis based on three-dimensional images obtained from on either peripheral or clinical computed tomography scanners.

The most dramatic declines in bone mineral after SCI are observed during the acute stages of injury (<1 year). At skeletal regions around the hip and knee, early rates of decline in integral vBMD have been reported as approximately 3.0 %/month [50, 51]. For comparison, reductions in vBMD during spaceflight are approximately 1.5 %/month [52], while those associated with normal aging are approximately 0.5–1.0 % per annum, depending on sex [53]. The rate of bone loss after SCI is greatest at the long-bone epiphyses (i.e., the proximal femur, distal femur, and proximal tibia) and progressively decreases moving towards the diaphyses [50, 51]. The epiphyseal regions are rich with trabecular bone leading some to postulate that bone is lost preferentially from trabecular as opposed to cortical bone [1, 54]. This is not the case as the loss of cortical bone from epiphyseal regions is typically equal if not greater than the loss of trabecular bone [50, 51, 55]. Our group has documented mean rates of bone mineral decline in trabecular- and cortical-specific bone as high as 4.4 and 5.4 %/month, respectively, at the distal femur and proximal tibia [51]. The loss of cortical bone after SCI takes place primarily through endocortical resorption with some intracortical remodeling observed years after injury; little to no periosteal resorption is ever observed [2, 50, 51, 55, 56•, 57, 58]. As the trabecular architecture progressively deteriorates and the endocortical surface expands, the cancellous regions become comprised primarily of marrow fat [56•, 59].

The rapid bone loss observed after SCI eventually slows down and reaches a new steady state anywhere from 2 to 8 years after injury [2, 56•, 60, 61], depending on the skeletal site and relative location within the bone. The temporal pattern of bone loss is nicely described by an exponential decay curve of the form: $y=Ae^{-bt}+C$, where A is the loss amplitude; b is the loss rate; C is the new steady state; and t is the time since SCI in years [2, 56•, 58]. New steady state values at the distal femur and proximal tibia are established anywhere between 2 and 4 years after injury [2, 56•, 60, 61], whereas those at the distal tibia are established anywhere between 5 and 7 years after injury [2, 60]. Both QCT and DXA studies have consistently illustrated that once the new steady state has been reached approximately 25 and 50 % of the bone mineral has been resorbed at the hip [1, 6, 7, 10, 62–65] and knee [1, 2, 5, 7, 10, 56•, 63, 64], respectively.

The reason that bone loss after SCI is both spatially and temporally distinct is not entirely clear, but may be attributed to different osteoclastogenic events mediating bone loss at different locations. Recent work in a murine botulinum-toxin-induced disuse model suggests an immediate resorption response at the epiphyses caused by basal osteoclast activity, followed by a later phase of bone resorption at the diaphyses associated with osteoclastogenisis within the marrow space [66•].

Bone Strength after SCI

Bone fractures are biomechanical events that occur when the applied load is greater than bone strength. When combined with the FE method, QCT images can serve as the basis for extremely accurate measures of bone strength. Specific details about the FE method and its clinical utility can be found in recent reviews of the topic in this journal [67, 68•]. In short, the FE method is a computational modeling technique that can be used to explicitly simulate the structural and material behavior of bone. FE models are completely patient specific with geometric and material property information being derived directly from the QCT image itself. These models are perhaps the most accurate of all computational models currently used in biomechanics as their outputs can be directly compared to measurements from in vitro cadaveric experimentation. When the correct algorithms are applied, FE models can account for more than 90 % of the variance in bone strength with an X=Y type of relationship [69, 70].

Reductions in FE-predicted bone strength after SCI are some 2–3 times greater than the observed reductions in bone mineral [45••, 71]. These changes in strength are heavily dependent on bone location and the applied mode of loading and are not necessarily correlated with changes in bone mineral [45••]. During the first few months of injury, proximal femoral strength in a fall type loading scenario decreases at a rate of 7 %/month [45••], which is twice the loss rate observed during spaceflight [72]. After 3.5 months of SCI, reductions in proximal femoral strength for some patients are on the order of that predicted for lifetime declines associated with aging [53]. Proximal tibial strength in torsion initially decreases at a rate of 4 %/month [71] and illustrates a similar exponential decline to that of bone mineral [56•]. The new steady state for torsional strength at the proximal tibia is reached after 2 years of injury at a magnitude 70 % lower than normal [56•]. The discrepancy in relative steady state values (i.e., 50 % less for bone mineral vs. 70 % less for bone strength) can be explained by the fact that bone strength is a multifactorial measure dependent not only on bone mass but also on geometry, mineral distribution, material properties, and mode of loading. Unlike basic densitometry measures, FE models are able to capture all of this information and account for their complex interaction. This makes FE-predicted bone strength an ideal outcome measure for a treatment or intervention [48, 49], specifically because it brings biomechanical relevance to any observed changes to bone.

It is important to note that even if bone mineral is restored to pre-SCI values following an initial loss, bone strength will not necessarily be fully recovered. Hypothetical treatments simulating a complete restoration of bone mineral density through pharmaceutical therapy suggest that bone strength will not be recovered if more than 10 % of the bone mineral has been lost after SCI prior to treatment [71]. Similar findings have been observed through computational simulations of age-related

osteoporosis [73–75]. What this suggests, in theory, is that simply restoring bone mineral back to pre-SCI levels through therapies that do not target the most "mechanically important" locations will not lead to a full recovery of bone strength. These findings also strongly support the use of early intervention after SCI to prevent bone loss. With bone loss rates of 3–5 %/month, postponing treatment for as few as 2 months may mean the inability to restore bone to an age-specific normal state, regardless of the rehabilitation program that can be initiated. This may be of particular relevance to those individuals with SCI who have the greatest potential for motor recovery.

Fracture Risk Assessment after SCI

Medical professionals have reported several barriers to bone loss therapy after SCI, one of which is the lack of a clinical fracture risk assessment tool specific to the SCI population [76]. Such as tool could be used to identify individuals in need of pharmacologic treatment or to objectively identify individuals that could safely participate in active therapy. The current fracture risk assessment tools for the general public would appear inadequate for people with SCI; the locations of routine fracture do not correspond between these two groups and bone density thresholds (T-scores) and the FRAX® tool developed for able-bodied populations would classify nearly all those with SCI at high risk for major osteoporotic fracture. Consequently, whereas some studies have illustrated significantly lower aBMD values at the hip in individuals with prevalent fractures compared to those without [10, 36], other studies have not observed this trend, either before [64] or after [32•] adjusting for completeness of injury.

A limited number of DXA protocols have been proposed for measuring aBMD at the knee in individuals with SCI [32•, 77–80]. Methods based on pre-existing algorithms (e.g., spine and forearm protocols) have illustrated high reliability [78–80], which is important for assessing longitudinal changes in, or making clinical recommendations based on, aBMD measurements. Cross-sectional studies have, quite consistently, demonstrated significant differences between knee aBMD in people with SCI and a history of fracture and those without fractures [10, 64, 81], even after adjusting for completeness of injury [32•]. Some of these studies suggest the existence of a "fracture threshold" corresponding to the value of a particular bone health measure above which fragility fractures rarely occur. For example, Garland et al. reported fracture thresholds of 0.78 g/cm^2 at the knee in males with SCI [81]. Fracture thresholds in individuals with SCI have also been reported using knee vBMD assessed with peripheral QCT. In patients with motor complete SCI, a trabecular vBMD of 114 mg/cm^3 defined fracture threshold at the distal femur, whereas 72 mg/cm^3 defined fracture threshold at the proximal tibia [33]. Peripheral QCT measurements of cortical thickness and surrogate measures of bone strength (e.g., mass-weighted moments of inertia) at the tibia have also illustrated significant differences between SCI individuals with and without prevalent fragility fracture [32•, 82].

In theory, patient-specific FE modeling should provide a more accurate prediction of fracture risk in the SCI population than QCT, which in turn should be more accurate than DXA. Indeed, research has consistently illustrated that information derived from FE models is associated with a substantial improvement in fracture strength prediction compared to DXA and QCT [69, 83, 84]. Evidence from large fracture surveillance studies in able-bodied adults suggests that FE-predicted bone strength is a better predictor of both prevalent [85] and incident [86] fractures when compared to measures from DXA. In these studies, the information derived from FE models remained a significant predictor of fracture risk even after controlling for aBMD.

In a small sample of 49 adults with SCI (1 to 50 years duration), we obtained DXA and clinical QCT scans at the knee to quantify aBMD and vBMD, respectively, at the distal femur and proximal tibia [87, 88]. Torsional strength at the proximal tibia was also quantified using patient-specific FE modeling. Participants self-reported the cause, location, and time of any lower-extremity fragility fractures sustained after SCI. The ability of aBMD, vBMD, and FE-predicted strength to classify groups with and without fractures was determined using discriminant analyses. Of the 49 participants, 14 had at least one prevalent fracture of the lower-extremity. FE-predicted strength (p=0.002), vBMD ($p \leq 0.014$), but not aBMD ($p \geq 0.195$), were significant discriminants of prevalent fractures. The overall classification accuracy for torsional strength at the proximal tibia was 74 %, while that for proximal tibial vBMD and distal femoral vBMD were 71 and 63 %, respectively. On average, FE-predicted strength and vBMD measures were 39 and 33 % lower, respectively, for individuals with fractures compared to individuals without fractures.

Although the findings above suggest that measures based on advanced imaging analysis may provide the most sensitive measure of fracture risk, these technologies have several shortcomings relative to DXA. DXA benefits from its relatively low-cost, availability, ease of use, and low radiation exposure. Clinical QCT is expensive, associated with a relatively high radiation dose, and cannot account for important aspects of bone quality including changes to trabecular microarchitecture and cortical porosity. Peripheral QCT shares similar benefits to DXA in terms of cost and radiation exposure and high-resolution peripheral scanners, which have not yet been widely used in SCI research and have the capability for direct microstructural measurements [89, 90]. The most recent high-resolution peripheral scanner (XtremeCTII; Scanco Medical) has a field of view and gantry length that would theoretically allow for measurements of bone mass, architecture, and strength at the knee, the most clinically relevant site for skeletal fracture in the SCI population.

Conclusions

Bone loss is a well-established secondary complication associated with SCI that leads to an increased risk of fracture similar or greater in magnitude to that observed in postmenopausal osteoporosis. Recent research based on QCT analysis has illustrated that bone loss after SCI is marked and bone mass decreases exponentially, reaching a new steady state as early as 2 years post injury at the most clinically relevant locations for fracture. Bone loss after SCI occurs primarily through a combination of trabecular and endocortical resorption, which dominates at the epiphyseal regions of lower-extremity long bones. This specific pattern of bone loss has large mechanical consequences, with reductions in FE-predicted bone strength being some 2–3 times greater than the observed reductions in bone mineral. It is important to note that simply restoring bone mineral after an initial loss may not necessarily result in a full recovery of bone strength.

Although fractures after SCI are not typically observed until 3 or more years of injury, clinicians responsible for acute treatment should be aware that only a short therapeutic window (a matter of weeks/months) exists after SCI, during which bone-specific intervention may attenuate reductions in mechanical integrity and ultimately prevent fragility fracture in this population. This statement is further emphasized by the lack of efficacy observed for therapeutic interventions to promote bone mineral accrual in individuals with chronic SCI [91–93]. As fractures after SCI have occurred during mechanical loading interventions designed to strengthen the musculoskeletal system, the acute stages of SCI represents the safest window for active treatment, and therapists should be cognizant of the associated risk of musculoskeletal loading in people with chronic SCI. The most effective interventions may be those targeting "mechanically important" skeletal regions, perhaps through combined pharmacologic and mechanical loading therapy. Therapeutic interventions targeting skeletal deconditioning associated with SCI may become even more imperative in the future as treatments for SCI are discovered and full recovery of mobility and function becomes a reality.

There is a critical need for a large prospective fracture surveillance study to examine the clinical efficacy of a fracture risk assessment tool specific to the SCI population. Fracture risk assessment may be used by medical professionals to identify individuals in need of pharmacologic treatment and help guide the safe implementation of rehabilitation protocols. Furthermore, identification of those individuals at greatest risk of fracture would allow for a more efficient and cost effective use of resources for management. Such as study should investigate the utility of DXA technology that is already clinically available. If these results are shown to be effective, these data can be rapidly disseminated to medical professionals, permitting the widespread adoption of such approaches. This work should also investigate the use of new advanced imaging and patient-specific FE modeling techniques, which should theoretically provide a more sensitive and accurate prediction of fracture risk after SCI and help validate DXA outcomes.

Compliance with Ethics Guidelines

Conflict of Interest Dr. Edwards declare they have no conflicts of interest to disclose

Dr. Schnitzer reports non-financial support from Eli LIlly, non-financial support from Novartis, outside the submitted work.

Human and Animal Rights and Informed Consent All studies by Dr. Edwards and Dr. Schnitzer involving animal and/or human subjects were performed after approval by the appropriate institutional review boards. When required, written informed consent was obtained from all participants.

References

Papers of particular interest, published recently, have been highlighted as:
- • Of importance
- •• Of major importance

1. Biering-Sorensen F, Bohr HH, Schaadt OP. Longitudinal study of bone mineral content in the lumbar spine, the forearm and the lower extremities after spinal cord injury. Eur J Clin Invest. 1990;20(3):330–5.
2. Eser P, Frotzler A, Zehnder Y, Wick L, Knecht H, Denoth J, et al. Relationship between the duration of paralysis and bone structure: a pQCT study of spinal cord injured individuals. Bone. 2004;34(5):869–80.
3. Jiang SD, Dai LY, Jiang LS. Osteoporosis after spinal cord injury. Osteoporos Int. 2006;17(2):180–92.
4. Alexandre C, Vico L. Pathophysiology of bone loss in disuse osteoporosis. Joint Bone Spine. 2011;78(6):572–6.
5. Garland DE, Adkins RH. Bone loss at the knee in spinal cord injury. Top Spinal Cord Inj Rehabil. 2001;6(3):37–46.
6. Sabo D, Blaich S, Wenz W, Hohmann M, Loew M, Gerner HJ. Osteoporosis in patients with paralysis after spinal cord injury. A cross sectional study in 46 male patients with dual-energy X-ray absorptiometry. Arch Orthop Trauma Surg. 2001;121(1–2):75–8.
7. Dauty M, Perrouin Verbe B, Maugars Y, Dubois C, Mathe JF. Supralesional and sublesional bone mineral density in spinal cord-injured patients. Bone. 2000;27(2):305–9.
8. Demirel G, Yilmaz H, Paker N, Onel S. Osteoporosis after spinal cord injury. Spinal Cord. 1998;36(12):822–5.
9. Vestergaard P, Krogh K, Rejnmark L, Mosekilde L. Fracture rates and risk factors for fractures in patients with spinal cord injury. Spinal Cord. 1998;36(11):790–6.
10. Zehnder Y, Luthi M, Michel D, Knecht H, Perrelet R, Neto I, et al. Long-term changes in bone metabolism, bone mineral density, quantitative ultrasound parameters, and fracture incidence after spinal cord injury: a cross-sectional observational study in 100 paraplegic men. Osteoporos Int. 2004;15(3):180–9.
11. Morse LR, Battaglino RA, Stolzmann KL, Hallett LD, Waddimba A, Gagnon D, et al. Osteoporotic fractures and hospitalization risk in chronic spinal cord injury. Osteoporos Int. 2009;20(3):385–92.

12. Gifre L, Vidal J, Carrasco J, Portell E, Puig J, Monegal A, et al. Incidence of skeletal fractures after traumatic spinal cord injury: a 10-year follow-up study. Clin Rehabil. 2014;28(4):361–9.
13. Craven BC, Robertson LA, McGillivray CF, Adachi JD. Detection and treatment of sublesional osteoporosis among patients with chronic spinal cord injury: proposed paradigms. Top Spinal Cord Inj Rehabil. 2009;14(4):1–22.
14. Biering-Sorensen F, Hansen B, Lee BS. Non-pharmacological treatment and prevention of bone loss after spinal cord injury: a systematic review. Spinal Cord. 2009;47(7):508–18.
15. Bryson JE, Gourlay ML. Bisphosphonate use in acute and chronic spinal cord injury: a systematic review. J Spinal Cord Med. 2009;32(3):215–25.
16. Maimoun L, Fattal C, Sultan C. Bone remodeling and calcium homeostasis in patients with spinal cord injury: a review. Metabolism. 2011;60(12):1655–63.
17. Jiang SD, Jiang LS, Dai LY. Mechanisms of osteoporosis in spinal cord injury. Clin Endocrinol (Oxf). 2006;65(5):555–65.
18. Battaglino RA, Lazzari AA, Garshick E, Morse LR. Spinal cord injury-induced osteoporosis: pathogenesis and emerging therapies. Curr Osteoporos Rep. 2012;10(4):278–85.
19. Dionyssiotis Y. Spinal cord injury-related bone impairment and fractures: an update on epidemiology and physiopathological mechanisms. J Musculoskelet Neuronal Interact. 2011;11(3):257–65.
20. Charmetant C, Phaner V, Condemine A, Calmels P. Diagnosis and treatment of osteoporosis in spinal cord injury patients: a literature review. Ann Phys Rehabil Med. 2010;53(10):655–68.
21. Chang KV, Hung CY, Chen WS, Lai MS, Chien KL, Han DS. Effectiveness of bisphosphonate analogues and functional electrical stimulation on attenuating post-injury osteoporosis in spinal cord injury patients—a systematic review and meta-analysis. PLoS One. 2013;8(11):e81124.
22. Cosman F, de Beur SJ, LeBoff MS, Lewiecki EM, Tanner B, Randall S, et al. Clinician's guide to prevention and treatment of osteoporosis. Osteoporos Int. 2014;25(10):2359–81.
23. Frotzler A, Cheikh-Sarraf B, Pourtehrani M, Krebs J, Lippuner K. Long-bone fractures in persons with spinal cord injury. Spinal Cord. 2015. doi:10.1038/sc.2015.74.
24. Comarr AE, Hutchinson RH, Bors E. Extremity fractures of patients with spinal cord injuries. Am J Surg. 1962;103:732–9.
25. Freehafer AA. Limb fractures in patients with spinal cord injury. Arch Phys Med Rehabil. 1995;76(9):823–7.
26. Rogers T, Shokes LK, Woodworth PH. Pathologic extremity fracture care in spinal cord injury. Top Spinal Cord Inj Rehabil. 2005;11(1):70–8.
27. Ragnarsson KT, Sell GH. Lower extremity fractures after spinal cord injury: a retrospective study. Arch Phys Med Rehabil. 1981;62(9):418–23.
28. Nottage WM. A review of long-bone fractures in patients with spinal cord injuries. Clin Orthop Relat Res. 1981;(155):65–70.
29.•• Carbone LD, Chin AS, Burns SP, Svircev JN, Hoenig H, Heggeness M, et al. Mortality after lower extremity fractures in men with spinal cord injury. J Bone Miner Res. 2014;29(2):432–9. **Population based, cohort study of male veterans with SCI demonstrating that fragility fractures and underlying comorbidities contribute to mortality after SCI**.
30. Krause JS, Carter RE, Pickelsimer EE, Wilson D. A prospective study of health and risk of mortality after spinal cord injury. Arch Phys Med Rehabil. 2008;89(8):1482–91.
31. Logan Jr WC, Sloane R, Lyles KW, Goldstein B, Hoenig HM. Incidence of fractures in a cohort of veterans with chronic multiple sclerosis or traumatic spinal cord injury. Arch Phys Med Rehabil. 2008;89(2):237–43.
32.• Lala D, Craven BC, Thabane L, Papaioannou A, Adachi JD, Popovic MR, et al. Exploring the determinants of fracture risk among individuals with spinal cord injury. Osteoporos Int. 2014;25(1):177–85. **Recent cross-sectional study demonstrating that aBMD at the knee and pQCT derived measures of tibial geometry are associated with fragility fractures after SCI**.
33. Eser P, Frotzler A, Zehnder Y, Denoth J. Fracture threshold in the femur and tibia of people with spinal cord injury as determined by peripheral quantitative computed tomography. Arch Phys Med Rehabil. 2005;86(3):498–504.
34. Wang CM, Chen Y, DeVivo MJ, Huang CT. Epidemiology of extraspinal fractures associated with acute spinal cord injury. Spinal Cord. 2001;39(11):589–94.
35. Frisbie JH. Fractures after myelopathy: the risk quantified. J Spinal Cord Med. 1997;20(1):66–9.
36. Lazo MG, Shirazi P, Sam M, Giobbie-Hurder A, Blacconiere MJ, Muppidi M. Osteoporosis and risk of fracture in men with spinal cord injury. Spinal Cord. 2001;39(4):208–14.
37. Black DM, Delmas PD, Eastell R, Reid IR, Boonen S, Cauley JA, et al. Once-yearly zoledronic acid for treatment of postmenopausal osteoporosis. N Engl J Med. 2007;356(18):1809–22.
38. Cummings SR, San Martin J, McClung MR, Siris ES, Eastell R, Reid IR, et al. Denosumab for prevention of fractures in postmenopausal women with osteoporosis. N Engl J Med. 2009;361(8):756–65.
39. Freehafer AA, Hazel CM, Becker CL. Lower extremity fractures in patients with spinal cord injury. Paraplegia. 1981;19(6):367–72.
40. Fournier A, Golerberg M, Green B, Brucker B, Petrofsky J, Eismont F, et al. Medical evaluation of the effects of computer assisted muscle stimulation in paraplegic patients. Orthopedics. 1984;7:1129–33.
41. Hartkopp A, Murphy RJ, Mohr T, Kjaer M, Biering-Sorensen F. Bone fracture during electrical stimulation of the quadriceps in a spinal cord injured subject. Arch Phys Med Rehabil. 1998;79(9):1133–6.
42. Keating JF, Kerr M, Delargy M. Minimal trauma causing fractures in patients with spinal cord injury. Disabil Rehabil. 1992;14:108–9.
43. Martínez AA, Cuenca J, Herrera A, Domingo J. Late lower extremity fractures in patients with paraplegia. Injury. 2002;33:583–6.
44. Brotherton SS, Krause JS, Nietert PJ. Falls in individuals with incomplete spinal cord injury. Spinal Cord. 2007;45(1):37–40.
45.•• Edwards WB, Schnitzer TJ, Troy KL. Reduction in proximal femoral strength in patients with acute spinal cord injury. J Bone Miner Res. 2014;29(9):2074–9. **Short-term prospective analysis demonstrating the rapid and disproportionate decline of bone strength after SCI in relation to bone mineral**.
46. Bousson V, Le Bras A, Roqueplan F, Kang Y, Mitton D, Kolta S, et al. Volumetric quantitative computed tomography of the proximal femur: relationships linking geometric and densitometric variables to bone strength. Role for compact bone. Osteoporos Int. 2006;17(6):855–64.
47. Manske SL, Liu-Ambrose T, Cooper DM, Kontulainen S, Guy P, Forster BB, et al. Cortical and trabecular bone in the femoral neck both contribute to proximal femur failure load prediction. Osteoporos Int. 2009;20(3):445–53.
48. Keaveny TM, Hoffmann PF, Singh M, Palermo L, Bilezikian JP, Greenspan SL, et al. Femoral bone strength and its relation to cortical and trabecular changes after treatment with PTH, alendronate, and their combination as assessed by finite element analysis of quantitative CT scans. J Bone Miner Res. 2008;23(12):1974–82.
49. Keaveny TM, McClung MR, Wan X, Kopperdahl DL, Mitlak BH, Krohn K. Femoral strength in osteoporotic women treated with teriparatide or alendronate. Bone. 2012;50(1):165–70.
50. Edwards WB, Schnitzer TJ, Troy KL. Bone mineral loss at the proximal femur in acute spinal cord injury. Osteoporos Int. 2013;24(9):2461–9.
51. Edwards WB, Schnitzer TJ, Troy KL. Bone mineral and stiffness loss at the distal femur and proximal tibia in acute spinal cord injury. Osteoporos Int. 2014;25(3):1005–15.

52. Lang T, LeBlanc A, Evans H, Lu Y, Genant H, Yu A. Cortical and trabecular bone mineral loss from the spine and hip in long-duration spaceflight. J Bone Miner Res. 2004;19(6):1006–12.
53. Keaveny TM, Kopperdahl DL, Melton 3rd LJ, Hoffmann PF, Amin S, Riggs BL, et al. Age-dependence of femoral strength in white women and men. J Bone Miner Res. 2010;25(5):994–1001.
54. Frey-Rindova P, de Bruin ED, Stussi E, Dambacher MA, Dietz V. Bone mineral density in upper and lower extremities during 12 months after spinal cord injury measured by peripheral quantitative computed tomography. Spinal Cord. 2000;38(1):26–32.
55. Rittweger J, Goosey-Tolfrey VL, Cointry G, Ferretti JL. Structural analysis of the human tibia in men with spinal cord injury by tomographic (pQCT) serial scans. Bone. 2010;47(3):511–8.
56.• Edwards WB, Simonian N, Troy KL, Schnitzer TJ. Reduction in torsional stiffness and strength at the proximal tibia as a function of time since spinal cord injury. J Bone Miner Res. 2015;30:1422–30. **Cross -sectional study demonstrating rapid decline of bone strength after SCI and the establishment of a new steady state within 2–3 years of injury**.
57. Modlesky CM, Slade JM, Bickel CS, Meyer RA, Dudley GA. Deteriorated geometric structure and strength of the midfemur in men with complete spinal cord injury. Bone. 2005;36(2):331–9.
58. Coupaud S, McLean AN, Allan DB. Role of peripheral quantitative computed tomography in identifying disuse osteoporosis in paraplegia. Skeletal Radiol. 2009;38(10):989–95.
59. Minaire P, Edouard C, Arlot M, Meunier PJ. Marrow changes in paraplegic patients. Calcif Tissue Int. 1984;36(3):338–40.
60. Frotzler A, Berger M, Knecht H, Eser P. Bone steady-state is established at reduced bone strength after spinal cord injury: a longitudinal study using peripheral quantitative computed tomography (pQCT). Bone. 2008;43(3):549–55.
61. Dudley-Javoroski S, Shields RK. Longitudinal changes in femur bone mineral density after spinal cord injury: effects of slice placement and peel method. Osteoporos Int. 2010;21(6):985–95.
62. Leslie WD, Nance PW. Dissociated hip and spine demineralization: a specific finding in spinal cord injury. Arch Phys Med Rehabil. 1993;74(9):960–4.
63. Garland DE, Adkins RH, Stewart CA, Ashford R, Vigil D. Regional osteoporosis in women who have a complete spinal cord injury. J Bone Joint Surg Am. 2001;83-A(8):1195–200.
64. Biering-Sorensen F, Bohr HH, Schaadt OP. Bone mineral content of the lumbar spine and lower extremities years after spinal cord lesion. Paraplegia. 1988;26:293–301.
65. Szollar SM, Martin EM, Sartoris DJ, Parthemore JG, Deftos LJ. Bone mineral density and indexes of bone metabolism in spinal cord injury. Am J Phys Med Rehabil. 1998;77(1):28–35.
66.• Ausk BJ, Huber P, Srinivasan S, Bain SD, Kwon RY, McNamara EA, et al. Metaphyseal and diaphyseal bone loss in the tibia following transient muscle paralysis are spatiotemporally distinct resorption events. Bone. 2013;57(2):413–22. **Animal study suggesting different osteoclastogenic events mediate metaphyseal and diaphyseal bone loss following paralysis**.
67. Edwards WB, Troy KL. Number crunching: how and when will numerical models be used in the clinical setting? Curr Osteoporos Rep. 2011;9(1):1–3.
68.• Carpenter RD. Finite element analysis of the hip and spine based on quantitative computed tomography. Curr Osteoporos Rep. 2013;11(2):156–62. **Recent review summarizing QCT based subject-specific FE modeling and its potential clinical utility**.
69. Edwards WB, Schnitzer TJ, Troy KL. Torsional stiffness and strength of the proximal tibia are better predicted by finite element models than DXA or QCT. J Biomech. 2013;46(10):1655–62.
70. Bessho M, Ohnishi I, Matsuyama J, Matsumoto T, Imai K, Nakamura K. Prediction of strength and strain of the proximal femur by a CT-based finite element method. J Biomech. 2007;40(8):1745–53.
71. Edwards WB, Schnitzer TJ, Troy KL. The mechanical consequence of actual bone loss and simulated bone recovery in acute spinal cord injury. Bone. 2014;60:141–7.
72. Keyak JH, Koyama AK, LeBlanc A, Lu Y, Lang TF. Reduction in proximal femoral strength due to long-duration spaceflight. Bone. 2009;44(3):449–53.
73. Guo XE, Kim CH. Mechanical consequence of trabecular bone loss and its treatment: a three-dimensional model simulation. Bone. 2002;30(2):404–11.
74. Silva MJ, Gibson LJ. Modeling the mechanical behavior of vertebral trabecular bone: effects of age-related changes in microstructure. Bone. 1997;21(2):191–9.
75. Pistoia W, van Rietbergen B, Ruegsegger P. Mechanical consequences of different scenarios for simulated bone atrophy and recovery in the distal radius. Bone. 2003;33(6):937–45.
76. Morse LR, Giangregorio L, Battaglino RA, Holland R, Craven BC, Stolzmann KL, et al. VA-based survey of osteoporosis management in spinal cord injury. PM R. 2009;1(3):240–4.
77. Morse LR, Lazzari AA, Battaglino R, Stolzmann KL, Matthess KR, Gagnon DR, et al. Dual energy x-ray absorptiometry of the distal femur may be more reliable than the proximal tibia in spinal cord injury. Arch Phys Med Rehabil. 2009;90(5):827–31.
78. McPherson JG, Edwards WB, Prasad A, Troy KL, Griffith JW, Schnitzer TJ. Dual energy X-ray absorptiometry of the knee in spinal cord injury: methodology and correlation with quantitative computed tomography. Spinal Cord. 2014;52:821–5.
79. Shields RK, Schlechte J, Dudley-Javoroski S, Zwart BD, Clark SD, Grant SA, et al. Bone mineral density after spinal cord injury: a reliable method for knee measurement. Arch Phys Med Rehabil. 2005;86(10):1969–73.
80. Bakkum AJ, Janssen TW, Rolf MP, Roos JC, Burcksen J, Knol DL, et al. A reliable method for measuring proximal tibia and distal femur bone mineral density using dual-energy X-ray absorptiometry. Med Eng Phys. 2014;36(3):387–90.
81. Garland DE, Adkins RH, Stewart CA. Fracture threshold and risk for osteoporosis and pathologic fractures in individuals with spinal cord injury. Top Spinal Cord Inj Rehabil. 2005;11:61–9.
82. de Bruin ED, Dietz V, Dambacher MA, Stussi E. Longitudinal changes in bone in men with spinal cord injury. Clin Rehabil. 2000;14(2):145–52.
83. Cody DD, Gross GJ, Hou FJ, Spencer HJ, Goldstein SA, Fyhrie DP. Femoral strength is better predicted by finite element models than QCT and DXA. J Biomech. 1999;32(10):1013–20.
84. Crawford RP, Cann CE, Keaveny TM. Finite element models predict in vitro vertebral body compressive strength better than quantitative computed tomography. Bone. 2003;33(4):744–50.
85. Melton 3rd LJ, Riggs BL, Keaveny TM, Achenbach SJ, Hoffmann PF, Camp JJ, et al. Structural determinants of vertebral fracture risk. J Bone Miner Res. 2007;22(12):1885–92.
86. Orwoll ES, Marshall LM, Nielson CM, Cummings SR, Lapidus J, Cauley JA, et al. Finite element analysis of the proximal femur and hip fracture risk in older men. J Bone Miner Res. 2009;24(3):475–83.
87. Edwards WB, Simonian N, Schnitzer TJ. Bone mineral density assessed by QCT, but not DXA, discriminates SCI patients with prevalent fragility fractures. Proceedings of the 4th Joint Meeting of the ISCoS and ASIA. 2015.
88. Edwards WB, Simonian N, Troy, KL, Schnitzer TJ. Discriminants of prevalent fragility fractures in chronic spinal cord injury. Proceedings of the American Society of Bone and Mineral Research Annual Meeting. 2014. http://www.asbmr.org/education/AbstractDetail?aid=221f59d8-978b-4a89-8734-201bd3bdd8c8.

89. Macdonald HM, Nishiyama KK, Kang J, Hanley DA, Boyd SK. Age-related patterns of trabecular and cortical bone loss differ between sexes and skeletal sites: a population-based HR-pQCT study. J Bone Miner Res. 2011;26(1):50–62.
90. Manske SL, Zhu Y, Sandino C, Boyd SK. Human trabecular bone microarchitecture can be assessed independently of density with second generation HR-pQCT. Bone. 2015;79:213–21.
91. Giangregorio LM, Webber CE, Phillips SM, Hicks AL, Craven BC, Bugaresti JM, et al. Can body weight supported treadmill training increase bone mass and reverse muscle atrophy in individuals with chronic incomplete spinal cord injury? Appl Physiol Nutr Metab. 2006;31(3):283–91.
92. Moran de Brito CM, Battistella LR, Saito ET, Sakamoto H. Effect of alendronate on bone mineral density in spinal cord injury patients: a pilot study. Spinal Cord. 2005;43(6):341–8.
93. Needham-Shropshire BM, Broton JG, Klose KJ, Lebwohl N, Guest RS, Jacobs PL. Evaluation of a training program for persons with SCI paraplegia using the Parastep 1 ambulation system: part 3. Lack of effect on bone mineral density. Arch Phys Med Rehabil. 1997;78(8):799–803.

ORIGINAL ARTICLE

JBMR®

Reduction in Torsional Stiffness and Strength at the Proximal Tibia as a Function of Time Since Spinal Cord Injury

W Brent Edwards,[1] Narina Simonian,[2] Karen L Troy,[3] and Thomas J Schnitzer[2]

[1]Human Performance Laboratory, Faculty of Kinesiology, University of Calgary, Calgary, Canada
[2]Department of Physical Medicine and Rehabilitation Feinberg School of Medicine, Northwestern University, Chicago, IL, USA
[3]Department of Biomedical Engineering, Worcester Polytechnic Institute, Worcester, MA, USA

ABSTRACT

Spinal cord injury (SCI) is characterized by marked bone loss and a high rate of low-energy fracture around regions of the knee. Changes in the mechanical integrity of bone after SCI are poorly defined, and a better understanding may inform approaches to prevent fractures. The purpose of this study was to quantify reductions in torsional stiffness and strength at the proximal tibia as a function of time since SCI. Sixty adults with SCI ranging from 0 to 50 years of duration and a reference group of 10 able-bodied controls received a CT scan of the proximal tibia. Measures of integral bone mineral were calculated for the total proximal tibia, and localized measures of cortical and trabecular bone mineral were calculated for the epiphysis, metaphysis, and diaphysis. Torsional stiffness (K) and strength (T_{ult}) for the total proximal tibia were quantified using validated subject-specific finite element models. Total proximal tibia measures of integral bone mineral, K, and T_{ult} decreased exponentially ($r^2 = 0.52$ to 0.70) and reached a new steady state within 2.1 to 2.7 years after SCI. Whereas new steady-state values for integral bone mineral and K were 52% to 56% ($p < 0.001$) lower than the reference group, the new steady state for T_{ult} was 69% ($p < 0.001$) lower than the reference group. Reductions in total proximal tibia measures occurred through a combination of trabecular and endocortical resorption, leaving a bone comprised primarily of marrow fat rather than hydroxyapatite. These findings illustrate that a short therapeutic window exists early (ie, 2 years) after SCI, during which bone-specific intervention may attenuate reductions in mechanical integrity and ultimately prevent SCI-related fragility fracture. © 2015 American Society for Bone and Mineral Research.

KEY WORDS: QCT; FINITE ELEMENT MODEL; DISUSE OSTEOPOROSIS; BONE STRENGTH; BONE FRACTURE

Introduction

Spinal cord injury (SCI) is a catastrophic, life-altering event associated with considerable physical, emotional, and financial burdens. In the United States and Canada, SCI affects some 350,000 people with an additional 16,000 new cases each year.[1,2] SCI is associated with a number of secondary complications, one of which is the marked loss of bone mineral, owing, in part, to a combination of mechanical disuse and neurogenic factors.[3] Bone loss after SCI is different from primary osteoporosis in that it occurs below the level of the neurological lesion with little to no loss at the spine or supralesional regions.[4–6] Lower-extremity bone loss is similar among quadriplegics and paraplegics,[4,7] with the greatest loss of bone mineral being observed around regions of the knee; it is not uncommon for 50% of the distal femur and proximal tibia integral bone mineral to be resorbed during the first 2 to 3 years of injury.[8,9]

The long-term clinical consequence of SCI-related bone loss is an increased rate of low-energy fracture, reported to be in the range of 1.2 to 3.4 per 100 patient years at risk.[6,10–13] This rate is similar to that of nonvertebral fractures occurring in postmenopausal osteoporotic women treated with placebo in antifracture efficacy trials.[14,15] It has been estimated that as many as 50% of individuals with SCI will experience a fragility fracture at some point during their life.[16] The impact these fractures have on quality of life, functional ability, and the utilization of medical resources has been well documented.[17] The most commonly reported causes of fracture after SCI are falls from wheelchairs, wheelchair transfers, and rolling over in bed.[6,17–19] Spiral fractures are frequently observed around the distal femur and proximal tibia,[20,21] implicating torsional loading as the principal mode of failure.

In a cross-sectional study, Eser and colleagues[9] used peripheral quantitative computed tomography (pQCT) to describe the time course and magnitude of bone loss after SCI at the distal epiphysis and midshaft of the femur and tibia. Depending on the parameter of interest, bone mineral decreased exponentially and reached a new steady state from 3 to 8 years postinjury.[9] The mechanical consequence of this

Received in original form December 19, 2014; revised form January 20, 2015; accepted February 3, 2015. Accepted manuscript online February 6, 2015.
Address correspondence to: W Brent Edwards, PhD, Human Performance Laboratory, Faculty of Kinesiology, University of Calgary, KNB 418, 2500 University Dr. NW, Calgary, AB T2N 1N4, Canada. E-mail: wbedward@ucalgary.ca

Journal of Bone and Mineral Research, Vol. 30, No. 8, August 2015, pp 1422–1430
DOI: 10.1002/jbmr.2474

bone loss remains unclear—bone stiffness and strength are multifactorial measures influenced by parameters such as bone size, shape, mineral distribution, and mode of loading. We have recently illustrated that reductions in bone strength during the first few months of SCI are two to three times greater than that predicted by reductions in bone mineral.[22,23] The magnitude and temporal pattern of bone stiffness and strength loss after chronic SCI, and whether or not a new steady state is eventually reached remains unknown.

Therefore, the purpose of this study was to quantify reductions in torsional stiffness and strength at the proximal tibia as a function of time since SCI. To this end, subject-specific finite element (FE) analyses were performed on a group of 60 participants with SCI of various injury durations. Exponential decay curves were used to describe changes in FE parameters after SCI, and new steady-state values were compared to a reference group of 10 able-bodied controls. QCT mineral analyses were also performed to elucidate the source of any changes in FE parameters. It is hoped that a better understanding of changes in the mechanical integrity of bone after SCI will inform approaches for the prevention and treatment of fragility fractures in the SCI population.

Subjects and Methods

Participants

Sixty adults with SCI ranging from 0 to 50 years of injury duration were recruited for this study (Table 1). Participants were of mixed neurological impairments and injury levels, but all had motor complete SCI (ie, American Spinal Injury Association [ASIA] Impairment Scale, category A or B) with the loss of ability to ambulate independently. All individuals were 21 years of age or older (to ensure a population with closed epiphyses) and selected with no regard to sex or ethnicity. Pregnant females and patients with current or recent (within 12 months) use of drugs that affect bone metabolism (eg, bisphosphonates, PTH, selective estrogen receptor modulators [SERMs]) were excluded from participation. A reference group of 10 healthy, able-bodied adults were also recruited that closely reflected the age, sex, weight, and stature distribution of the SCI group. All necessary Institutional Review Boards approved the study and participants provided written informed consent.

CT acquisition

The CT data were acquired for the nondominant knee (ie, contralateral to hand dominance) of each participant using a scan length that captured the proximal-most 15 cm of the tibia.

Table 1. Subject Characteristics

Parameter	Reference group	SCI group
Subjects,*n*	10	60
Females,*n*	3	15
Age (years)	36.6 ± 13.9	37.5 ± 13.5
Height (cm)	180.1 ± 11.2	176.4 ± 11.2
Weight (kg)	77.0 ± 12.7	75.3 ± 17.9
SCI duration (years)	N/A	12.4 ± 11.7; range, 0–50

The SCI and reference groups did not differ in terms of age ($p = 0.852$), height ($p = 0.327$), or weight ($p = 0.714$), as indicated by independent *t* tests.

SCI = spinal cord injury.

A few participants had fixation hardware, or other technical issues, at or near the nondominant knee, in which case CT data were acquired for the dominant knee. The CT scans were performed using a Sensation 64 Cardiac Scanner (Siemens Medical Systems, Forchheim, Germany) with acquisition settings of 120 kVp and 200 mAs. Images were reconstructed with a slice thickness of 1 mm and an in-plane pixel resolution of 0.352 mm. All scans included a phantom in the field of view with known calcium hydroxyapatite concentrations (QRM, Moehrendorf, Germany).

QCT mineral analysis

The QCT mineral analysis of the proximal tibia was performed using established protocols.[24,25] Briefly, CT data were imported to Mimics (Materialise, Leuven, Belgium) where images were realigned so that the axial direction corresponded to the long axis of the tibia; the mediolateral axis was defined by a line passing through the medial and lateral condyles of the tibia and the anteroposterior axis was oriented orthogonally. The CT Hounsfield units were converted to calcium hydroxyapatite density ρ_{ha} using a linear relationship established with the phantom. This process can result in negative ρ_{ha} values for voxels comprised primarily of marrow fat.[26]

Proximal tibias were segmented from the aligned images using a ρ_{ha} threshold of 0.15 g/cm^3 to identify the periosteal surface boundary. Integral volumetric bone mineral density (vBMD; g/cm^3) and bone mineral content (BMC; g) were calculated for the total proximal tibia, defined as all voxels within the periosteal surface boundary. The total proximal tibia included the first 30% of the entire lower-limb segment length, as measured from the proximal end of the bone. Segment lengths were estimated from self-reported stature using the proportionality constants of Drillis and Contini as cited by Winter.[27]

Local measures of compartmental bone were computed for epiphyseal, metaphyseal, and diaphyseal regions of the proximal tibia corresponding to 0% to 10%, 10% to 20%, and 20% to 30% of segment length, respectively. Cortical and trabecular compartments were identified as described.[24,25] Local measures of cortical vBMD and BMC were computed for the epiphysis, metaphysis, and diaphysis. Local measures of trabecular vBMD and BMC were only computed for the epiphysis and metaphysis. In addition, integral and cortical bone volumes (BV; cm^3) were quantified for each region and used as surrogate measures of periosteal and endosteal expansion, respectively.

FE analysis

Subject-specific FE modeling was used to predict torsional stiffness and strength of the proximal tibia as described.[23,25] The modeling procedures have been physically validated using cadaveric experimentation, and illustrated high coefficients of determination with in vitro torsional stiffness ($r^2 = 0.95$) and strength ($r^2 = 0.91$); regression slopes and intercepts were not significantly different from 1 and 0, respectively.[25]

Briefly, voxels making up the proximal tibia were converted to eight-node hexahedral elements with isotropic edge lengths of 1.5 mm using custom MATLAB (MathWorks, Natick, MA, USA) scripts. Elements were assigned inhomogeneous, anisotropic, nonlinear material properties based on bone apparent density ρ_{app} (ie, $\rho_{app} = \rho_{ha}/0.626$).[28] Pre-yield elastic moduli were

defined using a density-elasticity relationship specific to the proximal tibia:[29]

$$E_3 = 6570\rho_{app}^{1.37}$$

where E_3 is the axial modulus expressed in MPa, and ρ_{app} is expressed in g/cm^3. A constant anisotropy was assumed where:

$$\begin{aligned} &E_1 = 0.574 \cdot E_3; E_2 = 0.577 \cdot E_3; \\ &G_{12} = 0.195 \cdot E_3; G_{23} = 0.265 \cdot E_3; \\ &G_{31} = 0.216 \cdot E3;\ v_{12} = 0.427; v_{23} = 0.234;\ \text{and} \\ &v_{31} = 0.405. \end{aligned} \quad (30)$$

Subscripts 1 and 2 denote the mediolateral and anteroposterior directions, respectively.

Material nonlinearity was modeled as bilinear elastic–plastic with a postyield modulus that was 5% of the pre-yield modulus[31]; yield was defined using the quadratic Hill criterion for orthotropic materials. Yield strains were assumed to be isotropic in the normal (0.675%) and shear (1.215%) directions.[32] A torsional displacement was applied to surface nodes of the proximal-most 2 cm of bone and surface nodes distal to the proximal-most 13 cm of bone were constrained in translation; ie, 11 cm of bone was exposed. Torsional stiffness (K) was quantified from the linear portion of the torque-rotation curve and torsional strength (T_{ult}) was defined as the torque at which 10% of surface elements had failed.[25] Element failure was defined as a maximum principal strain greater than 1.41%.[32]

Curve fitting and statistical analysis

Curve fitting was performed with the Curve Fitting Toolbox in MATLAB (Natick, MA, USA) using identical procedures to those described by Eser and colleagues.[9] Exponential decay curves were fitted to QCT and FE parameters as a function of time since SCI:

$$y = Aexp(-bt) + C$$

where A is the loss amplitude; b, the loss rate; C, the new steady-state; and t the time in years. For each parameter, the mean time period corresponding to 95% of the decrease (t_{95}) was determined:

$$t_{95} = -\ln(0.05)/b$$

Means and SDs for each parameter were then quantified only for those subjects with an SCI duration $\geq t_{95}$; ie, subjects that had already reached the new steady state. Accounting for subject variance, the actual time to reach the new steady state (t_{ss}) was defined as the mean $\pm$ 0.5SD of the data for those subjects with an SCI duration $\geq t_{95}$:

$$t_{ss} - 1n(0.5 \times SD/A)/b.$$

The QCT and FE parameters for subjects with an SCI duration $\geq t_{ss}$ were compared to the reference group of 10 able-bodied adults using independent samples *t* tests. The *t* tests were performed in Microsoft Excel (Redmond, WA, USA) with the criterion alpha-level set to 0.05.

Results

Reductions in total proximal tibia measures of integral bone mineral (ie, vBMD and BMC), K, and T_{ult} were well-described using exponential decay curves as a function of time since SCI ($r^2 = 0.52$ to 0.70; Fig. 1). New steady-state values were

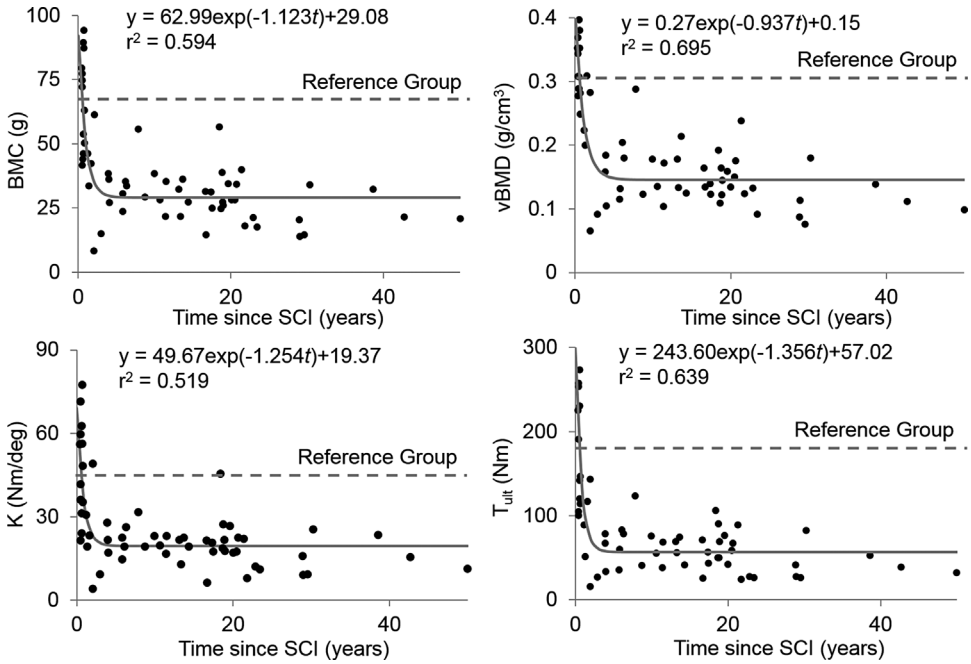

Fig. 1. Changes in total proximal tibia measures of integral bone mineral (BMC and vBMD) and FE predicted K and T_{ult} as a function of time since SCI. The solid line illustrates the line of best fit for an exponential decay curve (equation and r^2 also shown). The dashed line illustrates the mean value for the reference group of 10 ambulatory controls. FE = finite element; K = torsional stiffness; T_{ult} = torsional strength.

Table 2. Mean ± SD for Total QCT and FE Parameters of the Proximal Tibia for the Reference Group and SCI Group

Parameter	Reference group ($n = 10$)	SCI group $\geq t_{ss}$ ($n = 42$)	Difference (%)	t test (p)	t_{ss} (years)
Integral BMC (g)	65.0 ± 19.1	29.2 ± 9.5	−55.1	<0.001	2.3
Integral vBMD (g/cm^3)	0.31 ± 0.05	0.15 ± 0.04	−51.6	<0.001	2.7
K (Nm/deg)	44.2 ± 18.3	19.4 ± 7.2	−56.1	<0.001	2.1
T_{ult} (Nm)	184.7 ± 61.7	57.1 ± 23.9	−69.1	<0.001	2.2

Includes only subjects with an injury duration $\geq t_{ss}$.
FE = finite element; SCI = spinal cord injury; t_{ss} = time to reach the new steady state; K = torsional stiffness; T_{ult} = torsional strength.

established within 2.1 to 2.7 years after SCI, depending on the parameter (Table 2). Although new steady-state values for integral bone mineral and K were 52% to 56% ($p < 0.001$) lower than the reference group, the new steady state for T_{ult} was 69% ($p < 0.001$) lower than the reference group (Table 2). In general, the location of element failure went from being distributed across the total proximal tibia to being more localized toward the epiphysis, as bones went from strong to weak (Fig. 2).

Local measures of cortical and trabecular bone mineral decreased exponentially ($r^2 = 0.45$ to 0.70; Figs 3, 4) and reached a new steady state within 1.6 to 2.6 years after SCI, depending on the parameter (Table 3). All local measures of bone mineral after steady state were significantly lower than the reference group ($p < 0.001$); however, reductions in cortical vBMD were comparatively small. Negative mean values after steady state were observed for metaphyseal trabecular bone mineral, indicating a bone comprised primarily of marrow fat rather than hydroxyapatite.

Local measures of integral BV did not illustrate reductions after SCI (Table 3, Fig. 5). On the other hand, changes in local measure of cortical BV decreased exponentially ($r^2 = 0.35$ to 0.70) and reached a new steady state within 1.6 to 2.6 years after SCI (Table 3, Fig. 5). New steady-state values for cortical BV were 34% to 76% lower than the reference group, with relative differences decreasing in magnitude moving from the epiphysis toward the diaphysis.

Discussion

Bone loss after SCI and its clinical sequelae of fracture is a serious complication. The purpose of this study was to quantify reductions in torsional stiffness K and strength T_{ult} at the proximal tibia as a function of time since SCI. The findings from this study illustrated that changes in K and T_{ult} decreased exponentially and reached a new steady state within 2.1 to 2.2 years after SCI. Relative to a reference group of healthy able-bodied controls, the new steady state for K was similar in magnitude to that of integral bone mineral (ie, 52% to 56% lower than the reference group). However, the new steady state for T_{ult} was established at a value 69% lower than the reference group. The observed changes in K and T_{ult} were the result of localized resorption from both trabecular and cortical bone mineral compartments.

This study underscores the considerable influence that changes in bone mineral can have on bone mechanical integrity. The FE parameters based on clinical CT data that were investigated herein are dependent on multiple parameters including bone structure, mineral distribution, material properties, and mode of loading. It is interesting to note that new steady-state values relative to the reference group were similar among K and integral bone mineral, but substantially lower for T_{ult}. We observed a similar phenomenon following 3 to 5 months of acute SCI, in which relative reductions in K and integral bone

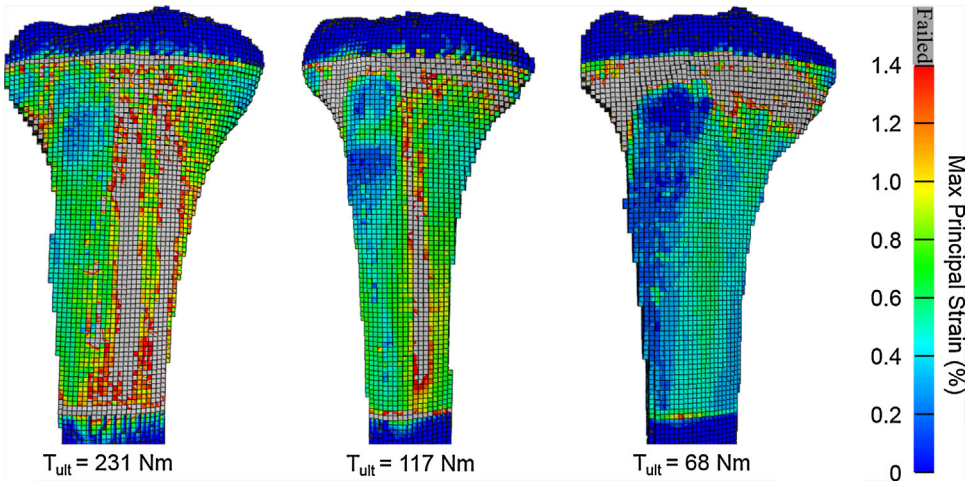

Fig. 2. Anteromedial views of representative FE models illustrating maximum principal strain and contours of surface element failure (ie, $\epsilon_{max} > 1.41\%$). The FE predicted T_{ult} corresponded to the torque at which 10% of the surface elements had failed. In general, the location of element failure went from being distributed across the total proximal tibia to being more localized toward the epiphysis, as bones went from strong to weak. FE = finite element; ϵ_{max} = maximum principal strain; T_{ult} = torsional strength.

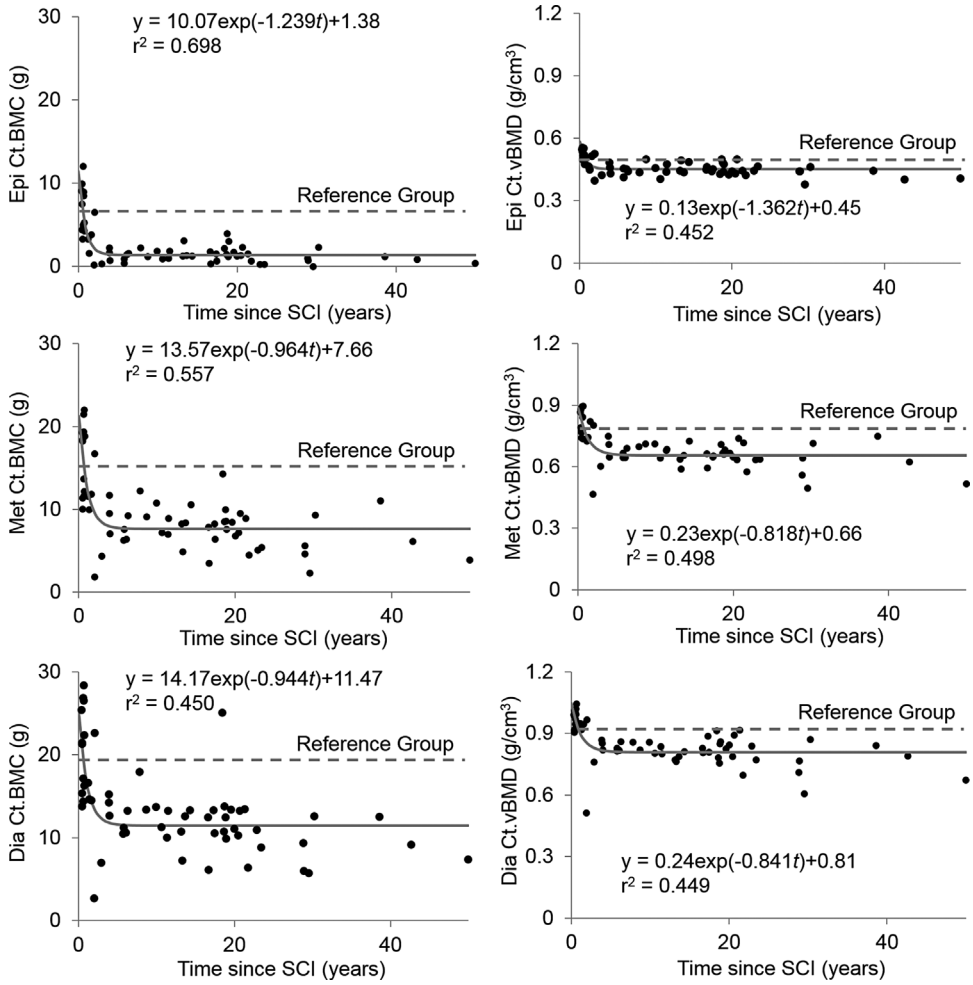

Fig. 3. Changes in local measures of Ct.BMC and Ct.vBMD at the proximal tibia epiphysis, metaphysis, and diaphysis as a function of time since SCI. The solid line illustrates the line of best fit for an exponential decay curve (equation and r^2 also shown). The dashed line illustrates the mean value for the reference group of 10 ambulatory controls. Ct = cortical; BMC = bone mineral content; vBMD = volumetric bone mineral density; Epi = epiphysis; Met = metaphysis; Dia = diaphysis.

mineral were similar in magnitude, whereas relative reductions in T_{ult} were approximately two times greater.[23] This discrepancy was explained by the fact that SCI-related bone loss had a larger influence on the post-yield rather than the pre-yield mechanical behavior in our models. Whether or not this is a true phenomenon can only be determined through cadaveric experimentation, but this would require a large number of specimens from individuals with SCI. We are aware of only one mechanical examination of cadaveric materials from the SCI population, for which the sample size was four.[33]

In this study, we limited our FE models to torsional loading because spiral fracture patterns are common in the SCI population[20,21] and this procedure has been validated using cadaveric experimentation.[25] More work is needed to determine if similar reductions in strength as a function of time since SCI would be observed under different modes of loading (eg, compression or bending). Nevertheless, the larger change in T_{ult} relative to other total proximal tibia measures suggests that FE models are able to capture information that is not readily obtained with simple measures of bone mineral. Indeed, evidence from large fracture surveillance studies in able-bodied adults suggests that FE-predicted strength is a better predictor of both prevalent[34] and incident[35] fractures when compared to DXA. In these studies, the information derived from FE models remained a significant predictor of fracture risk even after controlling for DXA assessed areal BMD. There is a critical need for a large, perhaps multisite, fracture surveillance study to examine the clinical efficacy of FE models as a fracture risk assessment tool for the SCI population. It would be valuable for such a study to precisely document and report the exact type and location of fracture, as our FE models suggest, at least for pure torsional loading, that fractures at the proximal tibia in chronic SCI (ie, after new steady state) would be localized to the epiphysis.

The observed reductions in total proximal tibia measures can be attributed to substantial resorption from both trabecular and cortical bone compartments. In terms of absolute bone mineral, the loss of trabecular BMC was greatest at the epiphysis and lowest at the metaphysis. Cortical BMC illustrated the opposite trend with absolute losses being lowest at the epiphysis and increasing in magnitude moving toward the diaphysis. In this regard, the greatest amount of trabecular and cortical bone

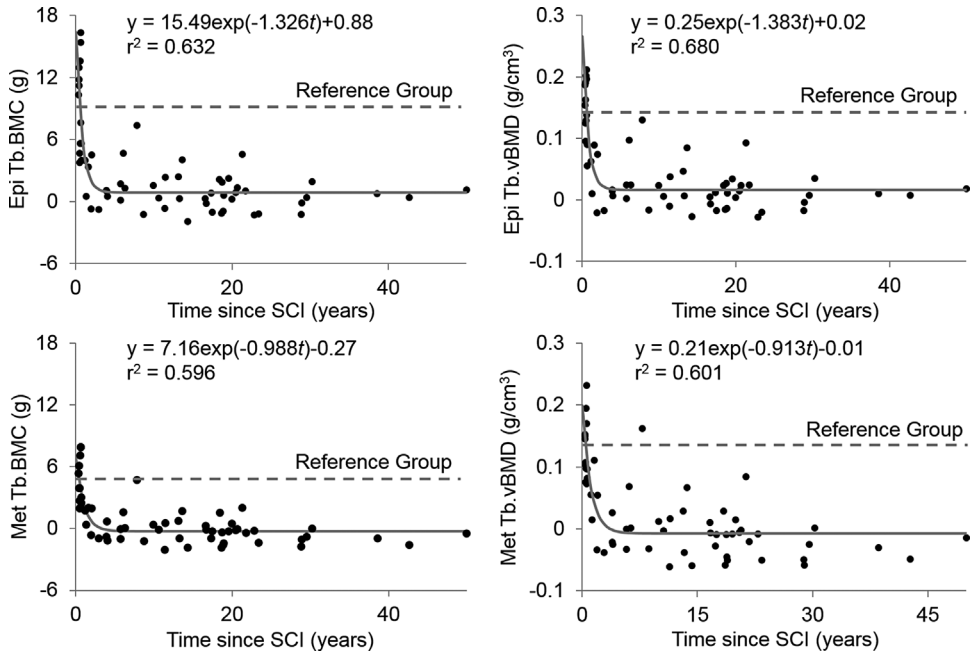

Fig. 4. Changes in local measures of Tb.BMC and Tb.vBMD at the proximal tibia epiphysis and metaphysis as a function of time since SCI. The solid line illustrates the line of best fit for an exponential decay curve (equation and r^2 also shown). The dashed line illustrates the mean value for the reference group of 10 ambulatory controls. Tb = trabecular; BMC = bone mineral content; vBMD = volumetric bone mineral density; Epi = epiphysis; Met = metaphysis.

resorption took place at regions having the highest initial trabecular and cortical BMC. Whereas measures of integral BV did not illustrate significant losses after SCI, cortical BV decreased exponentially to a new steady state that was 34% to 76% lower than the reference group, depending on location. In accordance with previous literature on mechanical disuse and bone loss,[9,24,36–38] these data suggest that cortical bone was lost primarily through endosteal rather than periosteal resorption, with some intracortical remodeling as indicated by small reductions in cortical vBMD.

Fragility fractures after SCI are not observed until approximately 3 years of injury,[6] corresponding nicely with our

Table 3. Mean ± SD for Local QCT Parameters of the Proximal Tibia for the Reference Group and SCI Group

Parameter	Reference group ($n = 10$)	SCI group $\geq t_{ss}$ (n)	Difference (%)	t test (p)	t_{ss} (years)
Epiphysis					
Integral BV (cm^3)	111.0 ± 19.1	106.6 ± 19.1 (60)	−4.0	0.501	n/a
Cortical BV (cm^3)	12.5 ± 4.1	3.0 ± 1.7 (42)	−76.0	<0.001	2.6
Cortical BMC (g)	6.5 ± 2.4	1.4 ± 0.8 (42)	−78.5	<0.001	2.6
Cortical vBMD (g/cm^3)	0.51 ± 0.02	0.45 ± 0.03 (44)	−11.8	<0.001	1.6
Trabecular BMC (g)	9.1 ± 3.4	0.9 ± 1.8 (42)	−90.1	<0.001	2.1
Trabecular vBMD (g/cm^3)	0.14 ± 0.04	0.02 ± 0.04 (43)	−85.7	<0.001	2.0
Metaphysis					
Integral BV (cm^3)	61.9 ± 14.8	56.4 ± 11.4 (60)	−8.9	0.173	n/a
Cortical BV (cm^3)	19.4 ± 4.3	11.5 ± 3.1 (42)	−40.7	<0.001	2.0
Cortical BMC (g)	15.1 ± 4.0	7.7 ± 2.5 (42)	−49.0	<0.001	2.5
Cortical vBMD (g/cm^3)	0.77 ± 0.05	0.66 ± 0.06 (42)	−14.3	<0.001	2.6
Trabecular BMC (g)	4.7 ± 3.9	−0.3 ± 1.3 (42)	−106.4	<0.001	2.4
Trabecular vBMD (g/cm^3)	0.13 ± 0.08	−0.01 ± 0.04 (42)	−107.7	<0.001	2.5
Diaphysis					
Integral BV (cm^3)	38.2 ± 8.3	36.4 ± 7.5 (60)	−4.7	0.495	n/a
Cortical BV (cm^3)	21.4 ± 5.5	14.1 ± 4.0 (44)	−34.1	<0.001	1.6
Cortical BMC (g)	19.7 ± 5.7	11.5 ± 3.5 (42)	−41.6	<0.001	2.2
Cortical vBMD (g/cm^3)	0.91 ± 0.05	0.81 ± 0.06 (42)	−11.0	<0.001	2.4

Includes only subjects with an injury duration $\geq t_{ss}$.
SCI = spinal cord injury; t_{ss} = time to reach the new steady state.

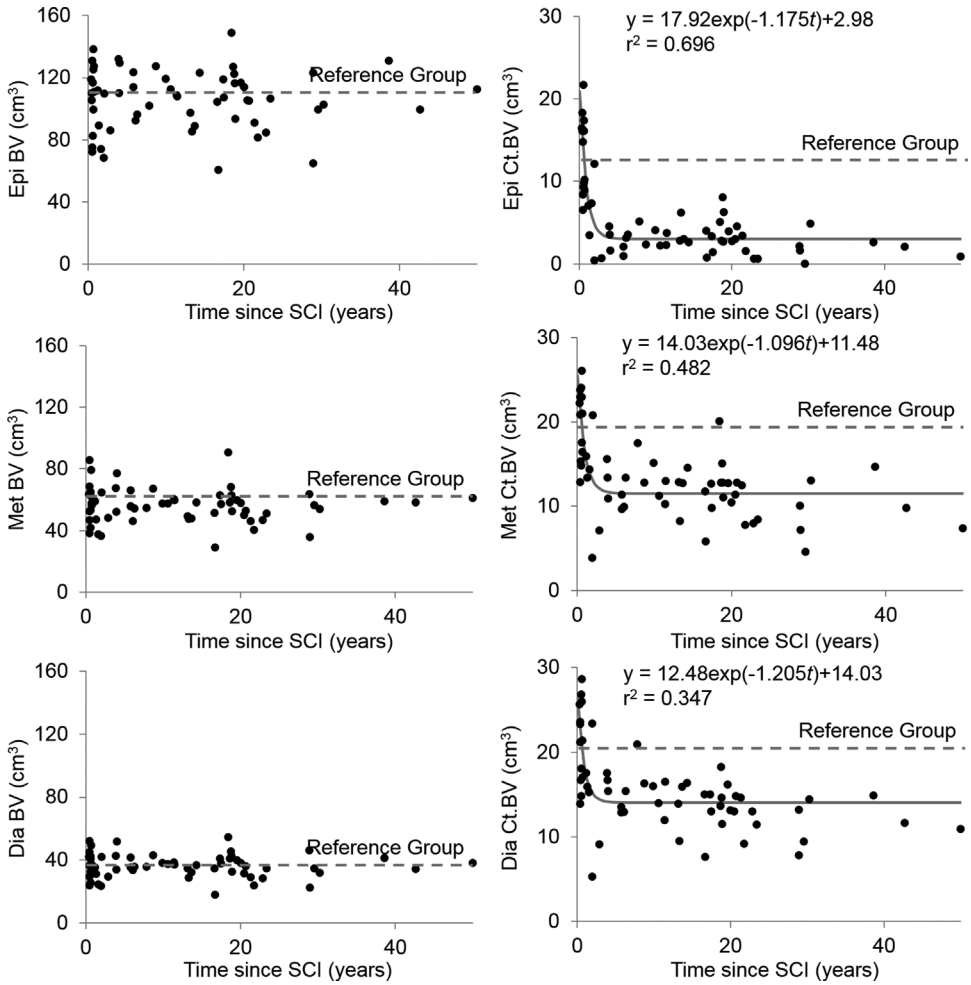

Fig. 5. Changes in local measures of integral and cortical bone volume at the proximal tibia epiphysis, metaphysis, and diaphysis as a function of time since SCI. Where significant, the solid line illustrates the line of best fit for an exponential decay curve (equation and r^2 also shown). The dashed line illustrates the mean value for the reference group of 10 ambulatory controls. Ct = cortical; Epi = epiphysis; Met = metaphysis; Dia = diaphysis.

measured time to reach a new steady state (ie, 1.7 to 2.7 years) when the proximal tibia is weakest. Previous research using DXA has reported new steady-state values of 1 to 3 years at the femoral neck and distal tibial epiphysis as well as a continuous decline beyond 10 years at the tibial diaphysis.[6] On the other hand, previous research using pQCT has reported new steady-state values of 2.9 to 4.1 years at the distal femoral epiphysis, and 4.8 to 6.8 years at the distal tibial epiphysis.[9] Although some of the discrepancy among these studies may be attributed to different densitometric techniques, the more likely explanation is that bone resorption following disuse is spatially and temporally distinct, even within individual bones.[39]

This study is limited by the cross-sectional design and heterogeneous sample used to characterize the magnitude and time course of bone mineral and strength loss after SCI. The cross-sectional analysis allowed us to estimate changes to bone that would occur up to an SCI duration of 50 years, which would be difficult, if not impossible, to quantify longitudinally. Although our sample was of mixed age, neurological impairment, and injury level, it should be emphasized that bone loss after SCI does not appear to depend on age,[40,41] and all participants were motor complete SCI (ie, ASIA Impairment Score A or B). Inherent to our curve-fitting analysis was the assumption that bone mineral and strength decreased exponentially and eventually reached a new steady state. These assumptions have been verified in a relatively small (ie, $n = 8$), short-term (ie, up to 4 years) longitudinal study,[8] but a key limitation of the exponential decay curve is that gradual changes to bone after steady state (eg, that associated with normal aging) were not quantified. On the other hand, any gradual changes after steady state would be considered negligible relative to the rapid and profound losses in bone observed during the first 2 years of SCI.

There are, of course, limitations associated with our estimations of torsional stiffness and strength. Clinical CT-based FE models cannot account for changes to bone microstructure (eg, trabecular architecture, tissue mineralization, collagen cross-linking, remodeling space), and as such the predicted reductions in K and T_{ult} as a function of time since SCI are likely conservative. As mentioned earlier, it is unclear if similar reductions in strength as a function of time since SCI would be observed under compressive or bending modes of loading. Pending the verification and validation of FE modeling procedures to predict compressive/bending strength at the

proximal tibia, we can only speculate that changes would be similar in magnitude based on our previous work illustrating comparable changes between QCT indices of torsional and compressive strength at the distal femur and proximal tibia after acute SCI.[24]

Conclusion

The results from this study illustrate that torsional stiffness and strength at the proximal tibia decrease exponentially and reach a new steady state within 2.2 years of SCI. Although the time to reach steady state was similar among total proximal tibia measures of integral bone mineral and strength, steady-state values for strength were considerably lower than bone mineral when expressed relative to an able-bodied reference group (ie, 69% versus 55% lower). Despite these rapid and profound losses to bone strength, there is currently no standard of care for SCI-related bone loss. It should be recognized that only a short therapeutic window exists after SCI, during which bone-specific intervention may attenuate reductions in mechanical integrity and ultimately prevent fragility fracture in this population. Because fractures after SCI have occurred during mechanical loading interventions designed to strengthen the musculoskeletal system,[42,43] the acute stages of SCI represents the safest window for active treatment, and therapists should be cognizant of the associated risk of musculoskeletal loading in people with chronic SCI.

Disclosures

WBE: Grant support: National Institutes of Health; Department of Defense; Investigator-initiated grant support: Merck & Co, Inc. KLT: Grant support: National Institutes of Health; Department of Defense; Investigator-initiated grant support: Merck & Co, Inc. TJS: Grant support: National Institutes of Health; Department of Defense; Department of Education; Industry-sponsored grant support: Eli Lilly & Co; Amgen, Inc.; Investigator-initiated grant support: Merck & Co, Inc; Zars Pharma, Inc. All authors state that they have no conflicts of interest.

Acknowledgments

This work was supported by grants from the National Institutes of Health (NIAMS, F32 AR061964 to WBE) and the Department of Defense (CDMRP, SC090010 to TJS). Its contents are solely the responsibility of the authors and do not necessarily represent the official views of the funding agencies.

Authors' roles: Study design: WBE, KLT, and TJS. Study conduct: WBE, NS, and TJS. Data collection: WBE, NS, and TJS. Data analysis: WBE. Data interpretation: WBE. Drafting manuscript: WBE. Revising manuscript content: NS, KLT, and TJS. Approving final version of manuscript: WBE, NS, KLT, and TJS. WBE takes responsibility for the integrity of the data analysis.

References

1. National Spinal Cord Injury Statistics Center. Spinal cord injury facts and figures. Birmingham, AL: National Spinal Cord Injury Statistics Center; 2010.
2. Noonan VK, Fingas M, Farry A, et al. Incidence and prevalence of spinal cord injury in Canada: a national perspective. Neuroepidemiology. 2012;38:219–26.
3. Jiang SD, Dai LY, Jiang LS. Osteoporosis after spinal cord injury. Osteoporos Int. 2006;17:180–92.
4. Dauty M, Perrouin Verbe B, Maugars Y, Dubois C, Mathe JF. Supralesional and sublesional bone mineral density in spinal cord-injured patients. Bone. 2000;27:305–9.
5. Garland DE, Adkins RH, Stewart CA, Ashford R, Vigil D. Regional osteoporosis in women who have a complete spinal cord injury. J Bone Joint Surg Am. 2001; 83-A: 1195–200.
6. Zehnder Y, Luthi M, Michel D, et al. Long-term changes in bone metabolism, bone mineral density, quantitative ultrasound parameters, and fracture incidence after spinal cord injury: a cross-sectional observational study in 100 paraplegic men. Osteoporos Int. 2004;15:180–9.
7. Demirel G, Yilmaz H, Paker N, Onel S. Osteoporosis after spinal cord injury. Spinal Cord. 1998;36:822–5.
8. Biering-Sorensen F, Bohr HH, Schaadt OP. Longitudinal study of bone mineral content in the lumbar spine, the forearm and the lower extremities after spinal cord injury. Eur J Clin Invest. 1990;20:330–5.
9. Eser P, Frotzler A, Zehnder Y, et al. Relationship between the duration of paralysis and bone structure: a pQCT study of spinal cord injured individuals. Bone. 2004;34:869–80.
10. Frisbie JH. Fractures after myelopathy: the risk quantified. J Spinal Cord Med. 1997;20:66–9.
11. Lazo MG, Shirazi P, Sam M, Giobbie-Hurder A, Blacconiere MJ, Muppidi M. Osteoporosis and risk of fracture in men with spinal cord injury. Spinal Cord. 2001;39:208–14.
12. Logan WC Jr, Sloane R, Lyles KW, Goldstein B, Hoenig HM. Incidence of fractures in a cohort of veterans with chronic multiple sclerosis or traumatic spinal cord injury. Arch Phys Med Rehabil. 2008;89: 237–43.
13. Ragnarsson KT, Sell GH. Lower extremity fractures after spinal cord injury: a retrospective study. Arch Phys Med Rehabil. 1981;62: 418–23.
14. Black DM, Delmas PD, Eastell R, et al. HORIZON Pivotal Fracture Trial. Once-yearly zoledronic acid for treatment of postmenopausal osteoporosis. N Engl J Med. 2007;356:1809–22.
15. Cummings SR, San Martin J, McClung MR, et al. FREEDOM Trial. Denosumab for prevention of fractures in postmenopausal women with osteoporosis. N Engl J Med. 2009;361:756–65.
16. Szollar SM, Martin EM, Sartoris DJ, Parthemore JG, Deftos LJ. Bone mineral density and indexes of bone metabolism in spinal cord injury. Am J Phys Med Rehabil. 1998;77:28–35.
17. Morse LR, Battaglino RA, Stolzmann KL, et al. Osteoporotic fractures and hospitalization risk in chronic spinal cord injury. Osteoporos Int. 2009;20:385–92.
18. Comarr AE, Hutchinson RH, Bors E. Extremity fractures of patients with spinal cord injuries. Am J Surg. 1962;103:732–9.
19. Freehafer AA, Hazel CM, Becker CL. Lower extremity fractures in patients with spinal cord injury. Paraplegia. 1981;19:367–72.
20. Keating JF, Kerr M, Delargy M. Minimal trauma causing fractures in patients with spinal cord injury. Disabil Rehabil. 1992;14:108–9.
21. Martínez AA, Cuenca J, Herrera A, Domingo J. Late lower extremity fractures in patients with paraplegia. Injury. 2002;33:583–6.
22. Edwards WB, Schnitzer TJ, Troy KL. Reduction in proximal femoral strength in patients with acute spinal cord injury. J Bone Miner Res. 2014;29:2074–9.
23. Edwards WB, Schnitzer TJ, Troy KL. The mechanical consequence of actual bone loss and simulated bone recovery in acute spinal cord injury. Bone. 2014;60:141–7.
24. Edwards WB, Schnitzer TJ, Troy KL. Bone mineral and stiffness loss at the distal femur and proximal tibia in acute spinal cord injury. Osteoporos Int. 2014;25:1005–15.
25. Edwards WB, Schnitzer TJ, Troy KL. Torsional stiffness and strength of the proximal tibia are better predicted by finite element models than DXA or QCT. J Biomech. 2013;46:1655–62.
26. Marshall LM, Lang TF, Lambert LC, Zmuda JM, Ensrud KE, Orwoll ES; Osteoporotic Fractures in Men (MrOS) Research Group. Dimensions and volumetric BMD of the proximal femur and their relation to age among older U.S. men. J Bone Miner Res. 2006;21:1197–206.

27. Winter DA. Biomechanics and motor control of human movement. 2nd ed. New York: John Wiley & Sons, Inc; 1990.
28. Dalstra M, Huiskes R, Odgaard A, van Erning L. Mechanical and textural properties of pelvic trabecular bone. J Biomech. 1993;26: 523–35.
29. Rho JY, Hobatho MC, Ashman RB. Relations of mechanical properties to density and CT numbers in human bone. Med Eng Phys. 1995;17:347–55.
30. Rho JY. An ultrasonic method for measuring the elastic properties of human tibial cortical and cancellous bone. Ultrasonics. 1996;34: 777–83.
31. Bayraktar HH, Morgan EF, Niebur GL, Morris GE, Wong EK, Keaveny TM. Comparison of the elastic and yield properties of human femoral trabecular and cortical bone tissue. J Biomech. 2004;37:27–35.
32. Rincon-Kohli L, Zysset PK. Multi-axial mechanical properties of human trabecular bone. Biomech Model Mechanobiol. 2009;8:195–208.
33. Lee TQ, Shapiro TA, Bell DM. Biomechanical properties of human tibias in long-term spinal cord injury. J Rehabil Res Dev. 1997;34: 295–302.
34. Melton LJ 3rd, Riggs BL, Keaveny TM, et al. Structural determinants of vertebral fracture risk. J Bone Miner Res. 2007;22:1885–92.
35. Orwoll ES, Marshall LM, Nielson CM, et al. Osteoporotic Fractures in Men Study Group. Finite element analysis of the proximal femur and hip fracture risk in older men. J Bone Miner Res. 2009;24:475–83.
36. Edwards WB, Schnitzer TJ, Troy KL. Bone mineral loss at the proximal femur in acute spinal cord injury. Osteoporos Int. 2013;24:2461–9.
37. Lang T, LeBlanc A, Evans H, Lu Y, Genant H, Yu A. Cortical and trabecular bone mineral loss from the spine and hip in long-duration spaceflight. J Bone Miner Res. 2004;19:1006-12.
38. Rittweger J, Simunic B, Bilancio G, et al. Bone loss in the lower leg during 35 days of bed rest is predominantly from the cortical compartment. Bone. 2009;44:612–8.
39. Ausk BJ, Huber P, Srinivasan S, et al. Metaphyseal and diaphyseal bone loss in the tibia following transient muscle paralysis are spatiotemporally distinct resorption events. Bone. 2013;57:413–22.
40. Bauman WA, Spungen AM, Wang J, Pierson RN Jr, Schwartz E. Continuous loss of bone during chronic immobilization: A monozygotic twin study. Osteoporos Int. 1999;10:123–7.
41. Wood DE, Dunkerley AL, Tromans AM. Results from bone mineral density scans in twenty-two complete lesion paraplegics. Spinal Cord. 2001;39:145–8.
42. Fournier A, Golerberg M, Green B, et al. Medical evaluation of the effects of computer assisted muscle stimulation in paraplegic patients. Orthopedics. 1984;7:1129–33.
43. Hartkopp A, Murphy RJ, Mohr T, Kjaer M, Biering-Sorensen F. Bone fracture during electrical stimulation of the quadriceps in a spinal cord injured subject. Arch Phys Med Rehabil. 1998;79: 1133–6.

Spinal Cord (2014) 52, 821–825

www.nature.com/sc

ORIGINAL ARTICLE

Dual energy X-ray absorptiometry of the knee in spinal cord injury: methodology and correlation with quantitative computed tomography

JG McPherson[1], WB Edwards[2], A Prasad[3], KL Troy[4], JW Griffith[5] and TJ Schnitzer[1]

Study Design: Comparison of diagnostic tests; methodological validation.
Objectives: Primary: to investigate the precision and reliability of a knee bone mineral density (BMD) assessment protocol that uses an existing dual energy X-ray absorptiometry (DXA) forearm acquisition algorithm in individuals with spinal cord injury (SCI). Secondary: to correlate DXA-based knee areal BMD with volumetric BMD assessments derived from quantitative computed tomography (QCT).
Setting: Academic medical center, Chicago, IL, USA.
Methods: Participants: a convenience sample of 12 individuals with acute SCI recruited for an observational study of bone loss and 34 individuals with chronic SCI who were screened for a longitudinal study evaluating interventions to increase BMD. Main outcome measures: root-mean-square standard deviation (RMS-SD) and intra/inter-rater reliability of areal BMD acquired at three knee regions using an existing DXA forearm acquisition algorithm; correlation of DXA-based areal BMD with QCT-derived volumetric BMD.
Results: The RMS-SD of areal BMD at the distal femoral epiphysis, distal femoral metaphysis and proximal tibial epiphysis averaged 0.021, 0.012 and 0.016 g cm $^{-2}$, respectively, in acute SCI and 0.018, 0.02 and 0.016 g cm $^{-2}$ in chronic SCI. All estimates of intra/inter-rater reliability exceeded 97% and DXA-based areal BMD was significantly correlated with QCT-derived volumetric BMD at all knee regions analyzed.
Conclusions: Existing DXA forearm acquisition algorithms are sufficiently precise and reliable for short-term assessments of knee BMD in individuals with SCI. Future work is necessary to quantify the reliability of this approach in longitudinal investigations and to determine its ability to predict fractures and recovery potential.
Sponsorship: This work was funded by the Department of Defense, grant number DOD W81XWH-10-1-0951, with partial support from Merck & Co, Inc.
Spinal Cord (2014) **52,** 821–825; doi:10.1038/sc.2014.122; published online 15 July 2014

INTRODUCTION

Spinal cord injury (SCI) has a major impact on systems that regulate bone metabolism,[1] and frequently leads to enhanced bone resorption and accelerated loss of bone mineral density (BMD).[1–4] Such a decrease in BMD compromises bone strength and predisposes individuals with SCI to fractures, even under minimally loaded conditions.[5,6] Although hip and spine BMD—known predictors of overall fracture risk in post-menopausal women—have been used as general monitors of bone loss post SCI,[7,8] the distal femur and proximal tibia are the most common sites of fracture in this population.[9,10] Indeed, bone loss at these locations is markedly greater than that at the hip and/or spine, rendering the knee a more sensitive and clinically relevant region in which to assess bone loss following SCI.[11,12]

Despite its potential clinical impact, quantification of BMD in skeletal regions surrounding the knee has yet to become routine practice. In part, this may stem from methodological issues surrounding the two most common means of BMD assessment, quantitative computed tomography (QCT) and dual energy X-ray absorptiometry (DXA). QCT provides a three-dimensional, or volumetric, measure of BMD (vBMD) that is largely free from artifacts that are potentially introduced by changes in limb position and/or ectopic bone formation as a consequence of heterotopic ossification. However, lingering concerns over the high costs and radiation exposure have limited the use of QCT to the research setting rather than in the clinic for routine BMD assessments in this population. DXA provides an alternative measure of BMD, but no widely accepted standardized protocol exists for computing knee BMD using DXA. In addition, its two-dimensional, or areal, measure of BMD (aBMD) may be subject to more artifacts from limb repositioning and/or ectopic new bone formation. Nevertheless, its widespread availability, low cost and minimal radiation exposure make DXA an appealing option. As a result, the development and validation of a DXA-based knee protocol would greatly facilitate

[1]Department of Physical Medicine and Rehabilitation, Feinberg School of Medicine, Northwestern University, Chicago, IL, USA; [2]Department of Kinesiology, University of Calgary, Calgary, AB, Canada; [3]Department of Medicine, Lincoln Medical Center, Weill Cornell Medical College, New York, NY, USA; [4]Department of Biomedical Engineering, Worcester Polytechnic Institute, Worcester, MA, USA and [5]Department of Medical Social Sciences, Northwestern University, Chicago, IL, USA
Correspondence: Professor TJ Schnitzer, Department of Physical Medicine and Rehabilitation, Feinberg School of Medicine, Northwestern University, 710 N. Lake Shore Drive, Suite #1020, Chicago, IL 60611, USA.
E-mail: tjs@northwestern.edu
Received 14 March 2014; revised 5 June 2014; accepted 18 June 2014; published online 15 July 2014

routine assessment and monitoring of knee BMD in both clinical and research settings.

A modest but growing body of research indicates that existing DXA acquisition algorithms intended for measurements of aBMD at other skeletal regions are capable of providing reliable estimates of distal femur and proximal tibia aBMD.[13–15] However, this finding has yet to be systematically investigated in individuals with SCI, where optimal limb positioning may be difficult to achieve and heterotopic ossification may be present. Consequently, the primary goal of this study was to establish the precision and intra-/inter-rater reliability of a standard DXA acquisition algorithm for assessment of distal femur and proximal tibia aBMD in both acute and chronic SCI populations. In addition, we quantified the correlation between DXA-based aBMD and QCT-based vBMD estimates in these cohorts, given that QCT is generally considered to be a more robust technique for BMD analysis.

MATERIALS AND METHODS

Study participants

Forty-six individuals with SCI were included in this study; all were recruited from the inpatient and outpatient populations at the Rehabilitation Institute of Chicago. Twelve of these individuals were recruited for an observational study of bone loss beginning acutely post SCI (acute cohort), whereas the remaining thirty-four individuals were screened for a longitudinal study evaluating interventions to increase BMD (chronic cohort; ClinicalTrials.gov identifier: NCT01225055) in chronic SCI. All participants were medically stable and non-ambulatory with an ASIA level of A, B or C at the time of study entry. Pregnant females and/or individuals with current or recent (within 12 months) use of drugs that affect bone metabolism were excluded from participation.

DXA acquisition and analysis

DXA scans were obtained using a Hologic QDR45400A instrument that was calibrated daily (Hologic, Inc., Bedford, MA, USA). A modified forearm algorithm was elected for scan acquisition,[15] with the imaging field comprising the distal two-third of the femur and the proximal one-third of the tibia (Figure 1). During scans, participants were placed in a supine position and the lower limb was stabilized in full extension. When possible, both knees were imaged, with duplicate scans per knee. The lower limb was repositioned and restabilized between adjacent scans on each knee.

Two individuals independently analyzed all DXA images, using the Hologic APEX software (Hologic, Inc.) to quantify aBMD. Three skeletal regions were analyzed that permitted direct comparison to a previously described QCT protocol:[3] two regions of interest (ROIs) corresponding to the first 0–10% and 10–20% of the femur as measured from the distal end (R1, R2, respectively), and one region corresponded the first 0–10% of the tibia as measured from the proximal end (R3; Figure 1). These regions anatomically correspond to the distal femoral epiphysis, distal femoral metaphysis and proximal tibial epiphysis. Segment lengths were estimated from self-reported stature using standard proportionality constants. This method of segment length was chosen in place of direct stature or segment measurement because of difficulties in reliably assessing these parameters in the SCI population.

QCT acquisition and analysis

Participants also received a QCT scan within 2 weeks of their corresponding DXA scans. All computed tomography images were acquired on the non-dominant knee using a Sensation 64 Cardiac scanner (Siemens Medical Systems, Forchheim, Germany; 120 kVp, 280 mAs, pixel resolution 0.352 mm, slice thickness 1 mm). Each scan was 30 cm in length and captured approximately 15 cm each of the distal femur and proximal tibia. All computed tomography scans included a phantom—placed on the side of, or underneath, the subjects' knee—with known calcium hydroxyapatite concentration (QRM, Moehrendorf, Germany). The phantom allowed conversion of computed tomography Hounsfield units into hydroxyapatite equivalent density for the calculation of vBMD. A single researcher performed all QCT analyses, using regions identical to those described for the DXA protocol; the reliability of this QCT analysis has been previously reported.[3]

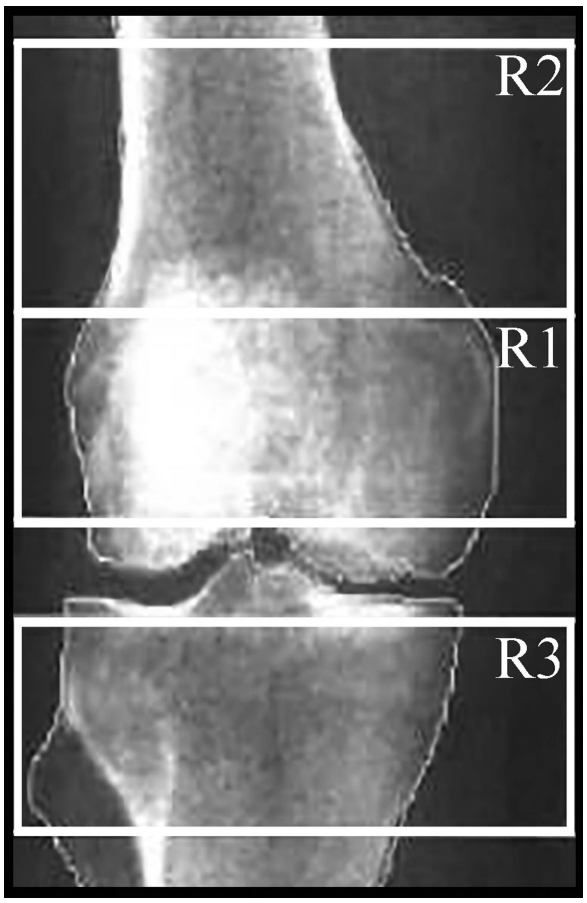

Figure 1 Anatomical regions of interest for DXA and QCT BMD analysis. R1: distal femoral epiphysis; R2: distal femoral metaphysis; R3: proximal tibial epiphysis.

Statistical analysis

Precision for each region of the DXA protocol was calculated using the short-term methodology recommended by International Society of Clinical Densitometry, defined as the root-mean-square standard deviation (RMS-SD), root-mean-square coefficient of variation (RMS-CV) and the least significant change.[16] Inter-rater reliability for each region of the DXA protocol was determined using intra-class correlation coefficients (Model type: two-way random, absolute agreement). In total, 42 pairs of knee scans (84 unique images) were used for precision and reliability analyses. The relationship between DXA-based aBMD and QCT-derived vBMD was calculated using Pearson's product-moment correlation on knees that had both DXA and QCT scans; duplicate single-rater aBMD values from DXA scans were averaged and correlated with QCT vBMD measurements. In total, 46 DXA-QCT image pairs were used for correlational analyses. SPSS Statistics software was used for all statistical calculations (SPSS, Armonk, NY, USA). Unless reported otherwise, data are reported as mean ± standard deviation, and considered significant at the $\alpha = 0.05$ level.

Statement of ethics. We certify that all applicable institutional and governmental regulations concerning the ethical use of human volunteers were followed during the course of this research. All studies were approved by the Northwestern University Institutional Review Board and all subjects provided written informed consent before participation.

RESULTS

General

Demographics and clinical information of the participants are provided in Table 1. The average age of acute SCI participants at the time of initial scan was 28.2 ± 13.0 years; the chronic SCI cohort averaged 41.9 ± 12.2 years. The mean time post-injury was 2.1 ± 0.7 months for the acute population and 196.9 ± 111.4 months for participants with chronic SCI. Mean DXA-based aBMD for acute and chronic SCI is presented in Table 2, with results from each rater displayed separately. Expectedly, mean aBMD levels in the acute SCI cohort were significantly greater than those of the chronic SCI population at each ROI.

Precision of the knee DXA protocol

A total of 42 pairs of DXA knee images were available for evaluation. The RMS-SD ($g\,cm^{-2}$), RMS-CV (%) and least significant change (%) of aBMD estimates are displayed in Table 3; data are parsed by rater, and presented separately for the acute and chronic subgroups, as well as the overall cohort. In the acute SCI group, RMS-CV values averaged 1.70%, 1.39% and 1.66% for the distal femur epiphysis, distal femur metaphysis and proximal tibia epiphysis, respectively; corresponding values for the chronic SCI cohort are: 3.12, 4.70 and 3.40%.

Reliability and reproducibility of the knee DXA measurements

Intra-class correlation coefficients were used to quantify the intra- and inter-rater reliability of DXA-based BMD assessments at each knee region. Reliability estimates were comparable in the acute and chronic SCI groups, with all intra-class correlation coefficients exceeding 0.97 (Table 4).

Table 1 Demographic and clinical data of study participants

	Acute SCI	*Chronic SCI*
Time post injury (months)	2.1 ± 0.7	196.9 ± 111.4
Age at injury (years)	28.2 ± 13.0	41.9 ± 12.2
Injury level distribution (%)		
Cervical	66.7	26.5
Thoracic	33.3	70.6
Lumbar	0	2.9
Gender distribution (%)		
F	33.3	21.6
M	66.7	79.4
Body mass index	24.1 ± 4.99	24.1 ± 5.98

Abbreviations: F, female; M, male; SCI, spinal cord injury.

Table 2 DXA-based mean bone mineral density for each knee region

	Acute SCI ($g\,cm^{-2}$)	*Chronic SCI ($g\,cm^{-2}$)*
Distal femur epiphysis		
Rater 1	1.255 ± 0.133	0.605 ± 0.183
Rater 2	1.255 ± 0.133	0.607 ± 0.181
Distal femur metaphysis		
Rater 1	0.927 ± 0.098	0.458 ± 0.175
Rater 2	0.927 ± 0.098	0.462 ± 0.173
Proximal tibia epiphysis		
Rater 1	0.944 ± 0.144	0.458 ± 0.131
Rater 2	0.944 ± 0.144	0.457 ± 0.130

Abbreviations: DXA, dual energy X-ray absorptiometry; SCI, spinal cord injury.

Correlation of QCT and DXA scans

Pearson product–moment correlations were used to quantify the strength of linear relationships between DXA-based aBMD and QCT-derived vBMD estimates for each knee region across the total cohort of study participants, and linear regression analysis was used to quantify the mapping between aBMD and vBMD at each site (Figure 2). Significant linear relationships between aBMD and vBMD were found at all ROIs.

DISCUSSION

This study quantified the precision and reliability of a DXA-based knee aBMD assessment protocol and the correlation between DXA-based aBMD and QCT-derived vBMD in both acute and chronic SCI populations. Across the knee ROIs analyzed in this investigation, the mean aBMD in individuals with acute SCI was approximately twice as high as the mean aBMD in individuals with chronic SCI (1.042 vs

Table 3 Estimates of precision for each knee region in acute, chronic and overall SCI cohorts

	Acute SCI	*Chronic SCI*	*Overall cohort*
Distal femur epiphysis			
Rater 1			
RMS-SD[a]	0.021	0.016	0.021
RMS-CV[b]	1.70	2.92	2.08
LSC[c]	4.70	8.08	5.80
Rater 2			
RMS-SD	0.021	0.019	0.023
RMS-CV	1.70	3.32	2.32
LSC	4.70	9.18	6.42
Distal femur metaphysis			
Rater 1			
RMS-SD	0.012	0.023	0.019
RMS-CV	1.39	5.53	2.61
LSC	3.85	15.31	7.22
Rater 2			
RMS-SD	0.0123	0.016	0.017
RMS-CV	1.39	3.86	2.25
LSC	3.85	10.70	6.24
Proximal tibia epiphysis			
Rater 1			
RMS-SD	0.016	0.018	0.021
RMS-CV	1.66	4.02	2.87
LSC	4.60	11.13	7.94
Rater 2			
RMS-SD	0.016	0.012	0.019
RMS-CV	1.66	2.77	2.63
LSC	4.60	7.67	7.28

Abbreviations: LSC, least significant change; RMS-CV, root-mean-square coefficient of variation; RMS-SD, root-mean-square standard deviation; SCI, spinal cord injury.
[a]RMS-SD: $g\,cm^{-2}$.
[b]RMS-CV: %.
[c]LSC: %.

0.508 g cm $^{-2}$). Measurements of aBMD also appeared to be more precise in the acute SCI cohort, with RMS-CV estimates of 1.70%, 1.39% and 1.66% for the distal femur epiphysis, distal femur metaphysis and proximal tibia epiphysis, respectively, compared with 3.12%, 4.70% and 3.40% in chronic SCI. However, the higher RMS-CV values in chronic SCI are largely attributable to this population's lower overall mean BMD rather than a systematic increase in RMS-SD. Indeed, for a similar absolute difference in aBMD, populations with lower mean aBMD will have higher RMS-CV estimates than those with higher mean aBMD, based on how RMS-CV is calculated. As such, if precision estimates—in particular, our estimates of least significant change—are expressed in units of aBMD (g cm $^{-2}$) rather than as a percentage of mean aBMD, similar results are found for both the acute and chronic cohorts: 0.059, 0.036 and 0.043 g cm $^{-2}$ for the acute subgroup and 0.049, 0.055 and 0.041 g cm $^{-2}$ in participants with chronic SCI.

Table 4 Estimates of intra- and inter-rater reliability in acute, chronic and overall SCI cohorts

	Acute SCI	*Chronic SCI*	*Overall*
	ICC	ICC	ICC
Distal femur epiphysis			
Inter-rater	0.992	0.991	0.999
Intra-rater (R1)	0.988	0.990	0.998
Intra-rater (R2)	0.988	0.986	0.998
Distal femur metaphysis			
Inter-rater	0.994	0.983	0.999
Intra-rater (R1)	0.992	0.975	0.998
Intra-rater (R2)	0.992	0.987	0.996
Proximal tibia epiphysis			
Inter-rater	0.996	0.991	0.998
Intra-rater (R1)	0.994	0.985	0.997
Intra-rater (R2)	0.994	0.993	0.997

Abbreviations: ICC, intra-class correlation coefficient; SCI, spinal cord injury.

Although few studies specifically designed to quantify the precision and reliability of DXA-based knee aBMD protocols exist in the literature, our estimates of these parameters are consistent with the available data. For example, Bakkum and colleagues have recently reported least significant knee BMD changes ranging from 0.047 to 0.077 g cm $^{-2}$ when using the existing Hologic DXA forearm acquisition algorithm.[15] Given that these estimates were derived from able-bodied individuals—a population markedly less prone to heterotopic ossification and repositioning difficulties than the SCI population tested here—it is particularly noteworthy that our precision and reliability estimates were comparable. In another investigation,Morse *et al.* reported RMS-CV values that were lower at the distal femur (3.01%) than the proximal tibia (5.91%) in a cohort of individuals with chronic SCI,[14] corresponding to least significant aBMD changes of 0.069 and 0.083 g cm $^{-2}$. Unlike the findings of Morse and colleagues, however, our estimates of precision and reliability were comparable at the distal femur and proximal tibia, potentially reflective of the different skeletal ROI used in the two studies and/or the consistency with which those ROI could be delineated. As a final comparison, estimates of least significant aBMD changes in post-menopausal women—another population where bone loss is prevalent—range from approximately 0.020 to 0.050 g cm $^{-2}$ at the traditional scanning sites of the hip and spine.[17,18]

Because the anatomical ROIs used in our DXA protocol were derived from a previously described QCT protocol,[3] we were able to quantify the strength and direction of a linear relationship between DXA-based aBMD measurements and their QCT-derived vBMD counterparts at each site (Figure 2). Importantly, the inclusion of individuals whose bone loss varied from negligible to severe (that is, acute SCI to chronic SCI) enabled these correlations to be examined over the full physiological range of knee BMDs, thus avoiding the well-known restriction of range problem in correlational analyses.[19] Our results revealed a significant, positive correlation between DXA-based aBMD and QCT-derived vBMD at each ROI, although the

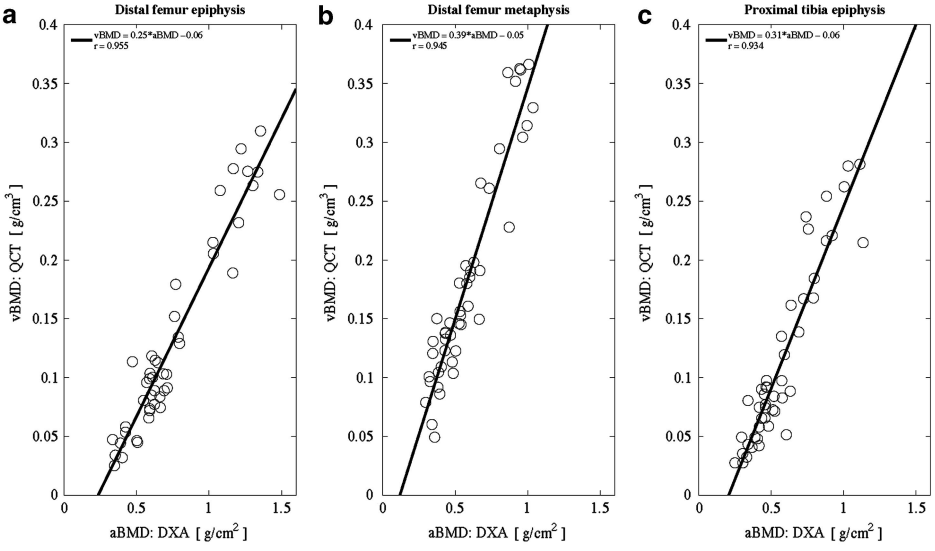

Figure 2 The relationship between QCT-derived vBMD vs DXA-based aBMD at each knee region. (**a**) Distal femur epiphysis; (**b**) distal femur metaphysis; (**c**) proximal tibia epiphysis. All panels: vertical axis reflects QCT-derived volumetric BMD (g cm $^{-3}$); horizontal axis reflects DXA-based areal BMD (g cm $^{-2}$); open circles: individual QCT-DXA pairs; bold line: linear regression fit of vBMD and aBMD.

slope of linear regression fits to these data varied slightly across sites. The difference in regression fits may be partly attributable to different proportions of cortical and trabecular bone at these sites. Nevertheless, the overall strength of each fit suggests that DXA-based aBMD and QCT-derived vBMD are linearly related and exhibit constant sensitivity over the relevant physiological operating range.

The primary limitation of this investigation is a potential underestimate of the effects of limb repositioning on precision and reliability. Although participants were repositioned between subsequent scans, a full dismount from the DXA table was not performed. Because changes in limb position and thus the imaging field can impact DXA-based aBMD estimates, it is possible that our performance metrics would have been lower had we more extensively repositioned each participant. In addition, although our estimates of short-term precision and reliability are highly clinically relevant, care should be taken when attempting to generalize these findings to situations in which long-term precision and reliability are more applicable. Finally, it should be reiterated that this study was performed using a Hologic Delphi DXA system, and consequently the absolute aBMD values reported herein will likely differ from aBMD measures computed using a GE Healthcare Lunar DXA system. Importantly, however, our protocol used Hologic Apex analysis software, which has comparable precision and reliability to GE Lunar Prodigy software.[20]

Despite the potential clinical importance of monitoring knee BMD post SCI and the ubiquity of DXA-based aBMD measurements at the hip and spine, DXA-based assessments of knee aBMD have yet to become standard clinical practice. Given that this lag is driven in part by the lack of commercially available DXA knee acquisition algorithms, a critical first step is to validate knee aBMD assessment protocols that use existing DXA acquisition algorithms as their basis. We believe that the protocol described herein mirrors what would be encountered in a typical clinic visit, and adequately reflects the challenges inherent to DXA-based knee aBMD assessments, particularly in individuals with SCI. In light of these challenges, it is important to again note that our estimates of precision and reliability were comparable at all knee regions. This consistency may allow clinicians to selectively choose which region(s) to analyze for each patient, potentially mitigating the impact of some postural or bony obstruction artifacts.

In summary, our results indicate that DXA is sufficiently precise and reliable to be used as the basis for routine monitoring of knee BMD post SCI. However, future work that systematically characterizes the sensitivity of DXA-based knee aBMD measurements to changes in limb position, ROI definitions and ectopic bone formation over short- and long-time scales will be essential to the design and interpretation of bone health interventions post SCI. And finally, as has been done previously for the hip and spine, determining the ability of DXA-based knee aBMD to predict fractures and subsequent recovery will be essential to establishing the full clinical utility of the technique.

DATA ARCHIVING

There were no data to deposit.

CONFLICT OF INTEREST

The authors declare no conflict of interest.

ACKNOWLEDGEMENTS

We thank Julia A Marks and Narina V Simonian for assistance with participant recruitment and data collection.

1 Dudley-Javoroski S, Shields RK. Regional cortical and trabecular bone loss after spinal cord injury. *J Rehabil Res Dev* 2012; **49**: 1365–1376.
2 Battaglino RA, Lazzari AA, Garshick E, Morse LR. Spinal cord injury-induced osteoporosis: pathogenesis and emerging therapies. *Curr Osteoporosis Rep* 2012; **10**: 278–285.
3 Edwards WB, Schnitzer TJ, Troy KL, Edwards WB, Schnitzer TJ, Troy KL. Bone mineral and stiffness loss at the distal femur and proximal tibia in acute spinal cord injury. *Osteoporos Int* 2013; **25**: 1005–1015.
4 Edwards WB, Schnitzer TJ, Troy KL. Bone mineral loss at the proximal femur in acute spinal cord injury. *Osteoporos Int* 2013; **24**: 2461–2469.
5 Zehnder Y, Luthi M, Michel D, Knecht H, Perrelet R, Neto I *et al.* Long-term changes in bone metabolism, bone mineral density, quantitative ultrasound parameters, and fracture incidence after spinal cord injury: a cross-sectional observational study in 100 paraplegic men. *Osteoporos Int* 2004; **15**: 180–189.
6 Fattal C, Mariano-Goulart D, Thomas E, Rouays-Mabit H, Verollet C, Maimoun L. Osteoporosis in persons with spinal cord injury: the need for a targeted therapeutic education. *Arch Phys Med Rehabil* 2011; **92**: 59–67.
7 Biering-Sorensen F, Bohr HH, Schaadt OP. Longitudinal study of bone mineral content in the lumbar spine, the forearm and the lower extremities after spinal cord injury. *Eur J Clin Invest* 1990; **20**: 330–335.
8 Leslie WD, Nance PW. Dissociated hip and spine demineralization: a specific finding in spinal cord injury. *Arch Phys Med Rehabil* 1993; **74**: 960–964.
9 Ragnarsson KT, Sell GH. Lower extremity fractures after spinal cord injury: a retrospective study. *Arch Phys Med Rehabil* 1981; **62**: 418–423.
10 Comarr AE, Hutchinson RH, Bors E. Extremity fractures of patients with spinal cord injuries. *Am J Surg* 1962; **103**: 732–739.
11 Gaspar AP, Lazaretti-Castro M, Brandao CM. Bone mineral density in spinal cord injury: an evaluation of the distal femur. *J Osteoporos* 2012; **2012**: 519754.
12 Garland DE, Adkins RH, Kushwaha V, Stewart C. Risk factors for osteoporosis at the knee in the spinal cord injury population. *J Spinal Cord Med* 2004; **27**: 202–206.
13 Shields RK, Schlechte J, Dudley-Javoroski S, Zwart BD, Clark SD, Grant SA *et al.* Bone mineral density after spinal cord injury: a reliable method for knee measurement. *Arch Phys Med Rehabil* 2005; **86**: 1969–1973.
14 Morse LR, Lazzari AA, Battaglino R, Stolzmann KL, Matthess KR, Gagnon DR *et al.* Dual energy X-ray absorptiometry of the distal femur may be more reliable than the proximal tibia in spinal cord injury. *Arch Phys Med Rehabil* 2009; **90**: 827–831.
15 Bakkum AJ, Janssen TW, Rolf MP, Roos JC, Burcksen J, Knol DL *et al.* A reliable method for measuring proximal tibia and distal femur bone mineral density using dual-energy X-ray absorptiometry. *Med Engin Phys* 2013; **36**: 387–390.
16 Baim S, Wilson CR, Lewiecki EM, Luckey MM, Downs Jr RW, Lentle BC. Precision assessment and radiation safety for dual-energy X-ray absorptiometry: position paper of the International Society for Clinical Densitometry. *J Clin Densitom* 2005; **8**: 371–378.
17 Lodder MC, Lems WF, Ader HJ, Marthinsen AE, van Coeverden SC, Lips P *et al.* Reproducibility of bone mineral density measurement in daily practice. *Ann Rheumat Dis* 2004; **63**: 285–289.
18 Ravaud P, Reny JL, Giraudeau B, Porcher R, Dougados M, Roux C. Individual smallest detectable difference in bone mineral density measurements. *J Bone Miner Res* 1999; **14**: 1449–1456.
19 Cohen J, Cohen P, West S, Aiken L. *Applied Multiple Regression/Correlation Analysis for the Behavioral Sciences*, 3rd edn. Mahwah, New Jersey, Lawrence Erlbaum Associates, 2003.
20 Fan B, Lewiecki EM, Sherman M, Lu Y, Miller PD, Genant HK *et al.* Improved precision with Hologic Apex software. *Osteoporos Int* 2008; **19**: 1597–1602.

Bone Mineral Density Assessed by QCT, But Not DXA, Discriminates SCI Patients with Prevalent Fragility Fractures

Introductions: Spinal cord injury (SCI) is characterized by marked bone loss and a high risk of fragility fracture around the knee. The objective of this study was to determine if BMD assessed by QCT and DXA can discriminate prevalent fracture after SCI.

Methods: Forty-nine adults with SCI (1 to 50 years duration) received DXA and QCT scans at the knee. DXA and QCT scans were used to quantify areal BMD (aBMD) and volumetric BMD (vBMD), respectively, at the distal femur and proximal tibia. Participants self-reported the cause, location, and time of any lower-extremity fragility fractures sustained after SCI. The ability aBMD and vBMD to classify groups with and without fractures was determined using discriminant analyses.

Results: Of the 49 participants, 14 had at least one prevalent fracture of the lower-extremity. The mean duration of SCI prior to first fragility fracture was 15.8 yrs (range 3-38 yrs). QCT measures of vBMD ($p \leq 0.014$), but not DXA measures of aBMD ($p \geq 0.195$), were significant discriminants of prevalent fractures. The overall classification accuracy for distal femoral vBMD and proximal tibial vBMD were 63.3%, and 71.4%, respectively. On average, vBMD measures were approximately 33.0% lower for individuals with fractures compared to individuals without fractures.

Conclusions: Fractures following SCI are a serious concern, but there is no validated fracture risk assessment tool specific to the SCI population. These results suggest that measurements obtained from QCT may provide a better assessment of fracture risk than those from DXA, but results should be confirmed in a larger sample.

Discriminants of Prevalent Fragility Fractures in Chronic Spinal Cord Injury

W. Brent Edwards, Karen L. Troy, Thomas J. Schnitzer

Spinal cord injury (SCI) is characterized by marked bone loss at regions below the neurological lesion. Within the first 2 to 3 years of SCI, some 50% of the bone mineral at the distal femur and proximal tibia is resorbed. The clinical consequence of this bone loss is a high incidence of low-energy fractures, most commonly observed at regions of the knee. Our purpose in this study was to identify and quantify clinical and bone-specific parameters that would discriminate prevalent fracture in chronic SCI.

Forty-two adults with SCI from 2.8 to 50.0 yrs of duration were recruited as part of a larger prospective intervention trial. Prior to treatment, computed tomography data were acquired for the proximal most 15cm of the non-dominant tibia. Bone mineral content (BMC) and volumetric bone mineral density (vBMD) were determined. Proximal tibia torsional strength (T_{ult}) was quantified using validated patient-specific finite element modeling procedures. The cause, location, and time of any lower-extremity fragility fractures that had occurred after SCI, and prior to treatment, were verified through medical records. The ability of SCI level and severity, BMC, vBMD, and T_{ult} to classify groups with and without fractures was determined using discriminant analyses.

Of the 42 participants, 14 had at least one prevalent fracture of the lower-extremity. The mean duration of SCI prior to first fracture was 15.8 yrs (range 3-38 yrs). SCI level and severity were not significant discriminants of individuals with and without prevalent fractures. The overall independent classification accuracy for T_{ult}, BMC, and vBMD were 71.4%, 69.0%, and 61.9%, respectively. On average, T_{ult} values were 33% lower for individuals with fractures compared to individuals without fractures (Figure 1). BMC and vBMD values were 25% and 17% lower for individuals with fractures compared to individuals without fractures.

In summary, measures of bone mineral and strength, but not SCI level or severity, were significant discriminators of prevalent lower-extremity fragility fractures in individuals with chronic SCI. These preliminary findings suggest a critical need for the assessment of bone mineral and strength after SCI, which is currently not the standard of care for this population. Recruitment for our prospective intervention trial is still ongoing, and we anticipate that larger numbers of participants will allow us to more accurately predict individuals at high risk for fracture after SCI.

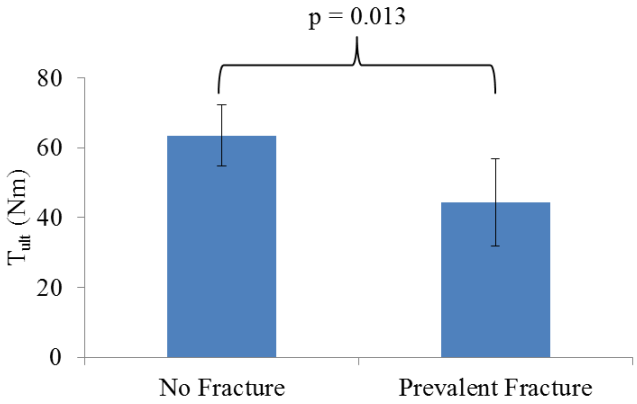

Figure 1. Mean (±95% CI) T_{ult} for the no fracture and prevalent fracture groups.

Increased marrow adipose tissue following Spinal Cord Injury

* Tiffiny Butler, Worcester Polytechnic Institute, US, Thomas Schnitzer, Northwestern University, UNITED STATES, William Edwards, University of Calgary, CA, Karen Troy, Worcester Polytechnic Institute, US

Spinal cord injury (SCI) all but eliminates loading from the paralyzed regions, resulting in rapid loss of both bone and muscle mass. Suboptimal loading from decreased muscle mass may alter the muscle-bone crosstalk resulting in increased medullary adiposity and decreased bone mass. Marrow adipose tissue (MAT) negatively regulates bone formation and may play a synergistic endocrine related role in the loss of bone following SCI. However, the exact function of MAT and its effect on other diseases is not well understood.

Our purpose was to determine factors related to tibial MAT accumulation following spinal cord injury in acute and chronic SCI subjects. We previously exploited clinical CT data to quantify visceral and intermuscular adipose tissue in the torso. Here, we established a similar technique to quantify MAT using quantitative CT. Computed tomography (CT) data of the proximal 15 mm of the non-dominant tibia were acquired on 49 subjects with acute (13 subjects) and chronic (36 subjects) SCI (41 male), age 22-65 years, duration of injury of 0–42.5 years. A calibration phantom with known hydroxyapetite concentrations was included in each scan and was used to establish a linear relationship between Hounsfield units (Hu) and tissue mineral density. Quantitative image analysis was performed to determine integral BMD (g/cm3) and MAT volume, defined as voxels within the periosteal envelope having Hu [-205 to -50]. Pearson's correlations were used to determine relationships between MAT volume (cm^3) and: BMD, duration of injury (years), age (years) and body mass (kg).

MAT volume was 31.1±23.9 cm3 for all subjects combined, 8.7±6.9 cm3 for acute subjects and 38.3± 22.9 cm3 for chronic subjects. MAT showed an inverse relationship with BMD ($r=-0.734$, $p<0.001$) and increased with duration of SCI ($r=0.51$, $p<0.001$; Figure 1) but not with age ($r=0.13$, $p=0.42$) or body mass ($r= -0.02$, $p=0.89$).

Although few studies have investigated changes in long bone MAT in individuals with SCI, others have linked increased marrow adiposity with decreased bone mineral density and cortical bone area. MAT and osteoblasts share common precursors, and low magnitude mechanical vibration has been shown to inhibit adipogenesis in mice. Similarly, resistance exercises and whole body vibration have been shown to prevent increases in vertebral marrow fat during prolonged bed rest. Further study of MAT in SCI patients may lead to improved understanding of the role MAT plays in bone health.

*** Presenting Authors(s):** Tiffiny Butler, Worcester Polytechnic Institute, US

ATTACHMENTS

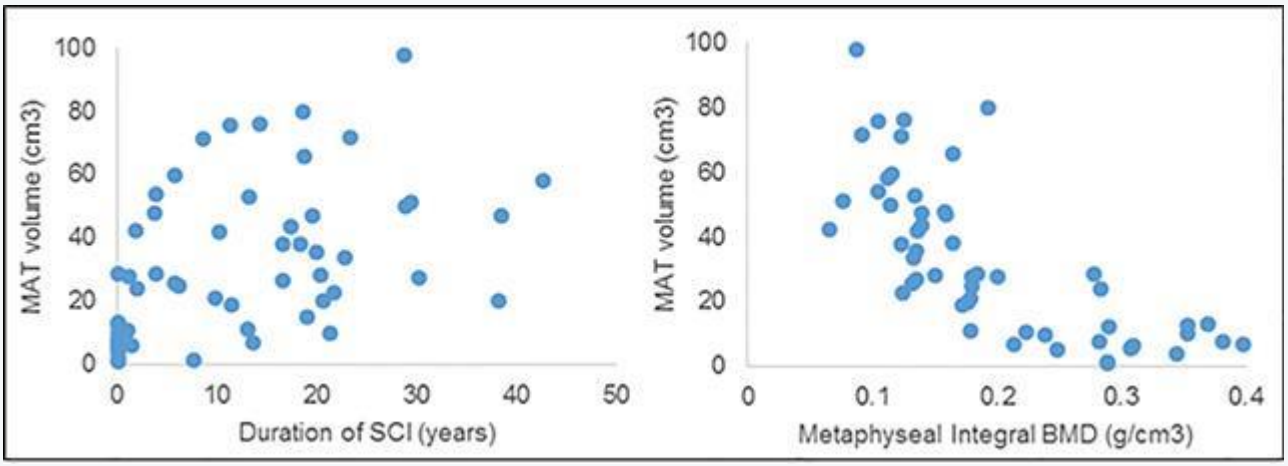

Figure 1: (a) MAT volume versus duration of spinal cord injury. (b) MAT volume versus integral BMD

Reduction in Proximal Tibia Compartmental Bone Mineral as a Function of Time since Spinal Cord Injury

W. Brent Edwards, Narina Simonian, Karen L. Troy, Thomas J. Schnitzer

Spinal cord injury (SCI) is characterized by marked bone loss at regions below the neurological lesion and a high rate of low-energy fracture. The greatest reductions in bone and highest incidence of fractures are observed around the knee. The temporal pattern of bone loss after SCI is poorly defined and a better understanding may inform approaches to prevent fractures. Our purpose was to quantify reductions to cortical and trabecular specific bone mineral at the epiphysis, metaphysis, and diaphysis of the proximal tibia as a function of time since SCI.

Sixty adults with SCI from 0 to 50 years of duration received computed tomography scans of the non-dominant proximal tibia. Cortical (Ct) and trabecular (Tb) volumetric bone mineral density (vBMD) and bone mineral content (BMC) were calculated for the epiphysis and metaphysis; Ct.vBMD and Ct. BMC were computed for the diaphysis. Exponential decay curves were used to describe changes in bone mineral as a function of time since SCI: $y = Aexp(-bt)+C$, where A is the loss amplitude; b, the loss rate; C, the new steady-state; and t the time in years. Measures of bone mineral after steady-state were compared to a reference group of 10 able-bodied adults.

Reductions in bone mineral with time since SCI were well described using exponential decay curves with r^2 ranging from 0.45-0.70. New steady-state values were established within 1.6 to 2.6 years after SCI, depending on the parameter (Table 1). All measures of bone mineral after steady-state were significantly lower than the reference group. Percent differences in Ct.vBMD were substantially smaller than all other parameters suggesting that cortical bone was lost primarily through endocortical rather than intracortical resorption. Negative mean values at the metaphysis were observed for Tb.vBMD and Tb.BMC in individuals with SCI, which indicates a proximal tibia comprised primarily of marrow fat rather than hydroxyapatite.

In summary, cortical and trabecular bone mineral decreased exponentially and reached a new steady state soon (2-3 years) after SCI. Although, percent changes in Tb.BMC were larger than that of Ct.BMC, absolute magnitudes of bone loss were similar amongst these compartments, which would lead to substantial reductions in fracture strength. Therefore, a therapeutic window exists early after SCI during which bone-specific intervention exists to aid in the prevention of SCI-related fragility fracture.

Funding: NIH-F32AR061964; US DOD -SC090010

Table 1. Means and standard deviations for bone parameters of the reference group and the SCI group (including only subjects with an injury duration ≥ time at steady-state (t_{ss}).

Parameter	Region	Reference group	SCI group after t_{ss}	Difference (%)	*t*-test (*p* value)	t_{ss} (years)
Ct.vBMD (g/cm^3)	Epiphysis	0.51±0.02	0.45±0.03	-13	<0.001	1.6
	Metaphysis	0.77±0.05	0.66±0.06	-15	<0.001	2.6
	Diaphysis	0.91±0.05	0.81±0.06	-11	<0.001	2.4
Tb.vBMD (g/cm^3)	Epiphysis	0.14±0.04	0.02±0.04	-88	<0.001	2.0
	Metaphysis	0.13±0.08	-0.01±0.04	-106	<0.001	2.5
Ct.BMC (g)	Epiphysis	6.5±2.4	1.4±0.8	-79	<0.001	2.6
	Metaphysis	15.1±4.0	7.7±2.5	-49	<0.001	2.5
	Diaphysis	19.7±5.7	11.5±3.5	-42	<0.001	2.2
Tb.BMC (g)	Epiphysis	9.1±3.4	0.9±1.8	-90	<0.001	2.1
	Metaphysis	4.7±3.9	-0.3±1.3	-105	<0.001	2.4

Correlation of DXA and QCT Imaging at the Knee in Adults with Spinal Cord Injury

Apoorv Prasad, M.D.[1]; W. Brent Edwards, Ph.D.[2]; Julia Marks, B.A.[3]; Karen L. Troy, Ph.D.[4]; Thomas J. Schnitzer, M.D., Ph.D.[3]

[1]Lincoln Hospital, New York, NY; [2]University of Calgary, Calgary, Canada; [3]Northwestern University Feinberg School of Medicine, Chicago, IL; [4]Worcester Polytechnic Institute, Worcester, MA.

Objective: To define and characterize a methodology for DXA imaging of bone at the distal femur and proximal tibia in individuals with spinal cord injury (SCI) and to correlate this methodology with QCT imaging

Design/Method: 52 individuals with either acute (11) or chronic (41) SCI participating in 2 studies of bone health had baseline DXA (Hologic QDR4500A) and QCT (Siemens Sensation 64) measurements of bone at the distal femur and proximal tibia. Three skeletal regions anatomically corresponding to the distal femur epiphysis, distal femur metaphysis and proximal tibia epiphysis were identified and analyzed by both DXA using a forearm algorithm and QCT using previously validated methodology. The precision, inter-rater reliability, RMS-SD and RMS-CV calculations for the DXA protocol were performed using the methodology recommended by ISCD. The BMD measurement by QCT and DXA were correlated using the Pearson's correlation analysis for each region.

Results: The average age (SD) of the chronic SCI population was considerably greater than the acute population (42.0±13.1 yr vs. 29.0±13.3 yr) and also had significantly lower BMD at all skeletal sites (e.g., 0.612±0.173 gm/cm^2 vs 1.237± 0.154 gm/cm^2 distal femoral epiphysis; $p<0.01$). There was high inter-rater reliability ($r>0.99$) at all skeletal sites. Regarding precision, the RMS-CV ranged from 1.6%-3.2% at knee skeletal sites in chronic SCI individuals and 2.0%-2.3% in those with acute injury. A strong, positive correlation was found between the BMD values of integral and trabecular bone compartments measured by QCT and the BMD values measured by DXA for all the three regions of the knee ($r \geq 0.74$, $p< 0.01$).

Conclusion: A new methodology for DXA measurement of bone at the knee for SCI individuals has been characterized; data obtained correlates strongly with QCT measurements at the same skeletal sites.

Support: DOD W81XWH-10-1-0951; Merck Inc.

Changes in Fracture Strength as a Function of Time since Spinal Cord Injury

W. Brent Edwards, Thomas J. Schnitzer, Karen L. Troy

Spinal cord injury (SCI) is characterized by marked bone loss at regions below the neurological lesion. The clinical consequence of this bone loss is a rate of low-energy fracture similar to that of post-menopausal osteoporotic women. The greatest reductions in bone are observed around regions of the knee. Within the first 2 to 3 years of SCI, some 50% of the bone mineral at the distal femur and proximal tibia is resorbed. Unfortunately, the mechanical consequence of this bone loss remains unclear. Therefore, our purpose was to quantify changes in fracture strength at the proximal tibia as a function of time since SCI.

Fifty one adults with SCI and a reference group of 5 able-bodied adults participated in this study. Computed tomography (CT) data were acquired for the proximal most 15cm of the non-dominant tibia. All CT images included a calibration phantom to convert CT attenuation to bone equivalent density. Bone mineral content (BMC) and volumetric bone mineral density (vBMD) were determined. Fracture strength of the proximal tibia loaded in torsion was quantified using validated patient-specific finite element modeling procedures. Exponential decay curves were used to describe changes in bone parameters and fracture strength as a function of time since SCI: $y = Aexp(-bt)+C$, where A is the loss amplitude; b, the loss rate; C, the new steady state; and t the time in years.

Reductions in BMC ($r^2 = 0.60$), vBMD ($r^2=0.71$), and fracture strength ($r^2=0.63$) with time since SCI were well described using exponential relationships. New steady state values in bone mineral and fracture strength were met within 2.0 – 2.4 years after SCI, depending on the parameter (Figure 1). Whereas, new steady state values for bone parameters were approximately 47% lower than the reference group, the new steady state value for fracture strength was approximately 63% lower than the reference group.

In summary, fracture strength of the proximal tibia decreased exponentially and reached a new steady state following SCI. Although the time to reach steady state was similar amongst bone parameters and fracture strength, steady state values for fracture strength were considerably lower than bone parameters when expressed relative to an able-bodied reference group. These data provide a more in-depth understanding of the mechanical consequence of bone loss after SCI, which ultimately may help in the prevention of SCI-related fragility fracture.

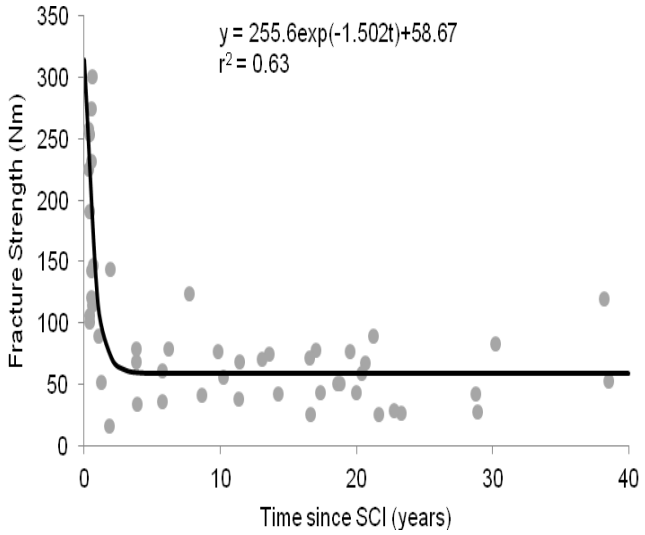
y = 255.6exp(-1.502t)+58.67
r2 = 0.63
Fracture Strength (Nm)
Time since SCI (years)
350
300
250
200
150
100
50
0
0
10
20
30
40

DXA vs QCT Imaging of the Knee in People with Spinal Cord Injury

Poster Sessions, Presentation Number: SA0435
Session: Poster Session I & Poster Tours
Saturday, October 5, 2013 12:00 PM - 2:00 PM, Baltimore Convention Center, Discovery Hall-Hall C

Apoorv Prasad, Northwestern University, William Edwards, University of Calgary, CA, Kristine Herrmann, Northwestern University, Danielle Barkema, Northwestern University, Narina Simonian, Northwestern University, Renita Yeasted, Northwestern University, Karen Troy, Worcester Polytechnic Institute, US, * Thomas Schnitzer, Northwestern University, UNITED STATES

Purpose: Bone loss is a common consequence of spinal cord injury (SCI) and is associated with a marked increase in fractures, particularly at sites around the knee. DXA measurement of the distal femur has been advocated to assess bone status though comparison with QCT has not been reported. This study was undertaken to compare DXA measurement to QCT imaging at the distal femur and proximal tibia.

Methods: A convenience sample of 31 individuals with SCI was studied; 11 were evaluated within 4 months of acute injury and the remainder had their injury for > 2yrs. Imaging of the knee by both QCT and DXA (Hologic QDR4500A) was accomplished within a 2 week timeframe in each individual. DXA of the knee was performed in duplicate. QCT data were analyzed to evaluate integral, trabecular and cortical BMD of three regions of the knees--distal femoral epiphysis, distal femoral metaphysis and proximal tibial epiphysis—per Drillis and Contini anthropometric proportionality constants (1966). DXA analysis utilized forearm software and a similar anatomic approach as the QCT analysis, with duplicate values for each region averaged. Correlation coefficients (Pearsons' r) were calculated using SPSS to evaluate correlations between site-specific DXA and QCT values.

Results: The study population was 67.7% male, average age 36.4±13.6 yr, duration of SCI 11.4±12.6 yr. There was excellent correlation between DXA and QCT trabecular and integral BMD measurements at the femoral epiphysis, femoral metaphysis and tibial epiphysis ($r>0.9$, $p<0.001$ for all), but weaker correlation between DXA and QCT cortical BMD values (Table 1).

Conclusions: A strong correlation exists between the DXA BMD and the integral and trabecular, but not the cortical, QCT values of the knee in all regions. QCT alone provides information regarding cortical bone status, important in assessing bone strength and fracture risk in SCI populations.

Disclosures: None

*** Presenting Authors(s):** Thomas Schnitzer, Northwestern University, UNITED STATES

ATTACHMENTS

Table 1. Pearson's r for Regions of the Knee: DXA vs QCT

	Integral	Trabecular	Cortical
Femoral epiphysis	0.96	0.96	0.39
Femoral metaphysis	0.93	0.92	0.53
Tibial epiphysis	0.94	0.94	0.73

Table 1